

# 1 On the Mechanistic Nature of Epistasis in a Canonical

## 2 *cis*-Regulatory Element

3  
4 Mato Lagator\*<sup>1</sup>, Tiago Paixão\*<sup>1</sup>, Nicholas H. Barton<sup>1</sup>, Jonathan P. Bollback<sup>1,2</sup>, Călin C. Guet<sup>1</sup>

5  
6 Affiliation: <sup>1</sup> IST Austria, 3400 Klosterneuburg, Austria

7 <sup>2</sup> Department of Integrative Biology, University of Liverpool, Liverpool, Merseyside, UK

### 8 9 ABSTRACT

10 **Understanding the relation between genotype and phenotype remains a major challenge.**  
11 **The difficulty of predicting individual mutation effects, and particularly the interactions**  
12 **between them, has prevented the development of a comprehensive theory that links**  
13 **genotypic changes to their phenotypic effects. We show that a general thermodynamic**  
14 **framework for gene regulation, based on a biophysical understanding of protein-DNA**  
15 **binding, accurately predicts the sign of epistasis in a canonical *cis*-regulatory element**  
16 **consisting of overlapping RNA polymerase and repressor binding sites. Sign and magnitude**  
17 **of individual mutation effects are sufficient to predict the sign of epistasis and its**  
18 **environmental dependence. Thus the thermodynamic model offers the correct null**  
19 **prediction for epistasis between mutations across DNA-binding sites. Our results indicate**  
20 **that a predictive theory for the effects of *cis*-regulatory mutations is possible from first**  
21 **principles, as long as the essential molecular mechanisms and the constraints these impose**  
22 **on a biological system are accounted for.**

26 INTRODUCTION

27 The interaction between individual mutations – epistasis – determines how a genotype maps  
28 onto a phenotype (Wolf et al. 2000; Phillips 2008; Breen et al. 2012). As such, it determines  
29 the structure of the fitness landscape (de Visser and Krug 2014) and plays a crucial role in  
30 defining adaptive pathways and evolutionary outcomes of complex genetic systems (Sackton  
31 and Hartl 2016). For example, epistasis influences the repeatability of evolution (Weinreich et  
32 al. 2006; Woods et al. 2011; Szendro et al. 2013), the benefits of sexual reproduction  
33 (Kondrashov 1988), and species divergence (Orr and Turelli 2001; Dettman et al. 2007).  
34 Studies of epistasis have been limited to empirical statistical descriptions, and mostly focused  
35 on interactions between individual mutations in structural proteins and enzymes (Phillips  
36 2008; Starr and Thornton 2016). While identifying a wide range of possible interactions  
37 (Figure 1), these studies have not led to a consensus on whether there is a systematic bias on  
38 the sign of epistasis (Lalic and Elena 2012; Kussell 2013; Valenich and Gore 2013; Kondrashov  
39 and Kondrashov 2014), a critical feature determining the ruggedness of the fitness landscape  
40 (Poelwijk et al. 2011). Specifically, it is only when mutations are in sign epistasis that the  
41 fitness landscape can have multiple fitness peaks - a feature that determines the number of  
42 evolutionary paths that are accessible to Darwinian adaptation (de Visser and Krug 2014).  
43 Furthermore, even a pattern of positive or negative epistasis has consequences for important  
44 evolutionary questions such as the maintenance of genetic diversity (Charlesworth et al.  
45 1995) and the evolution of sex (Kondrashov 1988; Otto and Lenormand 2002). While the  
46 absence of such a bias does not reduce the effect of epistasis on the response to selection, it  
47 does demonstrate that predicting epistasis remains elusive.

48

49 Scarcity of predictive models of epistasis comes as no surprise, given that most experimental  
50 studies focused on proteins. The inability to predict structure from sequence, due to the  
51 prohibitively large sequence space that would need to be experimentally explored in order to

52 understand even just the effects of point mutations (Maerkl and Quake 2009; Shultzaberger  
53 et al. 2012), let alone the interactions between them, prevents the development of a  
54 predictive theory of epistasis (Lehner 2013; de Visser and Krug 2014). In fact, the only  
55 predictive models of epistasis focus on tractable systems where it is possible to connect the  
56 effects of mutations to the underlying biophysical and molecular mechanisms of the  
57 molecular machinery (Dean and Thornton 2007; Lehner 2011); namely, RNA sequence-to-  
58 shape models (Schuster 2006), and models of metabolic networks (Szathmáry 1993). Even  
59 though these studies have provided accurate predictions of interactions between mutations,  
60 applying their findings to address broader evolutionary questions remains challenging. For  
61 RNA sequence-to-shape models, the function of a novel phenotype (new folding structure) is  
62 impossible to determine without experiments. In addition, this approach cannot account for  
63 the dependence of epistatic interactions on even simple variations in cellular environments,  
64 which are known to affect epistasis (Flynn et al. 2013; Caudle et al. 2014). On the other hand,  
65 metabolic network models are limited to examining the effects of large effect mutations, like  
66 deletions and knockouts, and lack an explicit reference to genotype.

67

68 In order to overcome the limitations of existing theoretical approaches to predicting  
69 epistasis, we focused on bacterial regulation of gene expression as one of the simplest model  
70 systems in which the molecular biology and biophysics of the interacting components are  
71 well understood. We analyze the effects of mutations in a prokaryotic *cis*-regulatory element  
72 (CRE) – the region upstream of a gene containing DNA binding sites for RNA polymerase  
73 (RNAP) and transcription factors (TFs). As such, we study a molecular system where an  
74 interaction between multiple components, rather than a single protein, determines the  
75 phenotype. Promoters that are regulated by competitive exclusion of RNAP by a repressor  
76 are particularly good candidates for developing a systematic approach to understanding  
77 epistasis as, in contrast to coding regions as well as more complex CREs and activatable

78 promoters (Garcia et al. 2012), the phenotypic effects of mutations in binding sites of RNAP  
79 and repressor are tractable due to their short length and the well-understood biophysical  
80 properties of protein-DNA interactions ( Bintu et al. 2005b; Saiz and Vilar 2008; Vilar 2010).  
81 Understanding the effects of point mutations in the *cis*-element on the binding properties of  
82 RNAP and TFs allows for the construction of a realistic model of transcription initiation (Bintu  
83 et al. 2005a; Kinney et al. 2010), while providing a measurable and relevant phenotype - gene  
84 expression level - for the analysis of epistasis.

85

## 86 RESULTS

87 Here we studied epistasis between point mutations in the canonical lambda bacteriophage  
88 CRE (Ptashne 2011) (Fig.2). We employ a fluorescent reporter protein that is under the  
89 control of the strong lambda promoter  $P_R$  (Fig.2a), which is fully repressed by an inducible TF,  
90 CI (Fig.2b). RNAP and CI have overlapping binding sites in this CRE, and hence compete for  
91 binding. We created a library of 141 random double mutants in the CRE, with all their  
92 corresponding single mutants (Supplementary File 1). This design allows us to calculate  
93 epistasis between the mutations in the *cis*-regulatory element in two environments: in the  
94 absence of CI, when only RNAP determines expression; and in the presence of CI when the  
95 two proteins compete for binding.

96

### 97 **Most double mutants change the sign of epistasis between the two environments**

98 Throughout we assume a multiplicative model of epistasis, which defines epistasis as a  
99 deviation of the observed double mutant expression level (relative to the wildtype) from the  
100 product of the relative single mutant expression levels (Phillips 2008). It should be noted that  
101 there is no *a priori* expectation for the sign of epistasis, even if most mutations are  
102 deleterious: epistasis denotes only deviations from the expected phenotype of the double  
103 mutant, and can be either positive or negative (Figure 1). First, we measured expression



104 levels in the absence of CI (Fig.3 – Figure Supplement 1a, Fig.3 – Figure Supplement 2a). We  
105 observe that the majority of double mutants are in negative epistasis (Fig.3a) — the observed  
106 double mutant expression level is lower than the multiplicative expectation based on single  
107 mutant expression levels (Pearson's  $\chi^2_{1,112}=43.82$ ,  $p<0.0001$ ). Specifically, we observe  
108 negative epistasis in 83% of 113 mutants that display statistically significant epistasis, while  
109 28 double mutants do not display significant epistasis (Fig.3a, Fig.3 – Source Data 1).

110

111 Next we estimated epistasis at high CI concentration, when gene expression depends on the  
112 competitive binding between RNAP and CI (Fig.3b, Fig.3 – Figure Supplement 1b, Fig.3 –  
113 Figure Supplement 2b, Fig.3 – Source Data 1). In a repressible promoter, the effects of  
114 mutations on the binding of the two proteins have opposite effects on gene expression — a  
115 reduction in RNAP binding leads to a decrease in gene expression, while a reduction in CI  
116 binding leads to higher expression levels. By comparing epistasis between two environments  
117 – absence of CI and high CI concentration – we find that the 141 tested random double  
118 mutants show a strong dependence on the environment (ANOVA testing for a GxGxE  
119 interaction:  $F_{1,280}=21.77$ ;  $p<0.0001$ ), in line with previous observations in another bacterial  
120 regulatory system (Lagator et al. 2015). Interestingly, 58% of double mutants display a  
121 change in the sign of epistasis between the two environments (Fig.4). Especially prevalent is a  
122 switch from negative epistasis in the absence of CI, to positive epistasis in its presence (Fig.4).  
123 Strikingly, the proportion of double mutants exhibiting reciprocal sign epistasis (when the  
124 sign of the effect of each mutation changes in the presence of the other mutation) is greater  
125 in the presence (66%) than in the absence (8%) of CI (Supplementary File 2). This difference  
126 likely arises from the molecular architecture of a repressible strong promoter. Mutations  
127 affect the binding of both DNA binding proteins, but in the presence of CI the effect on the  
128 binding of RNAP is only unmasked when CI does not fully bind, a scenario that is more likely  
129 in the presence of two mutations.

130

131 **Generic model of a simple CRE**

132 In order to understand these observations, we created a model of gene regulation that relies  
133 on statistical thermodynamical assumptions to model the initiation of transcription, originally  
134 developed to describe gene regulation by the lambda bacteriophage repressor CI (Ackers et  
135 al. 1982). Importantly, our model is generic, as it does not consider the details of any specific  
136 transcription factors involved in regulation. Instead, we model competitive binding between  
137 two generic transcription factors that share a single binding site (Fig.5a). The binding of one  
138 of these TFs leads to an increase in the gene expression level, in a manner similar to the  
139 function of a typical RNAP or an activator. The other is a repressor molecule, the binding of  
140 which has a negative effect on gene expression level, achieved by blocking access of the  
141 activator to its cognate binding site. In order to draw a parallel to our experimental system,  
142 we refer to these two TFs in the generic model as ‘RNAP’ and ‘repressor’, without actually  
143 relying on any specific properties of the two molecules, such as CI dimerization, or  
144 cooperative binding of CI dimers to multiple operator sites.

145

146 In the thermodynamic model of transcription, each DNA-binding protein is assigned a binding  
147 energy ( $E_i$ ) to an arbitrary stretch of DNA. In our formulation, we assume that each position  
148 along the single DNA binding site under consideration contributes additively to the global  
149 free binding energy – an assumption found to be accurate at least for a few mutations away  
150 from a reference sequence (Vilar 2010). These energy contributions can be determined  
151 experimentally (Kinney et al. 2010), and are typically represented in the form of an energy  
152 matrix. Given a set of DNA binding proteins (specifically, their energy matrices) and a  
153 promoter sequence, a Boltzmann weight can be assigned to any configuration of these  
154 proteins on the promoter. The Boltzmann weight is proportional to the probability of finding  
155 the system in each of the possible configurations. By assigning a Boltzmann weight to all

156 configurations, one can calculate the probability of finding the system in a particular state (a  
 157 set of configurations sharing a common property). Specifically, one can calculate the  
 158 probability of finding the system in a configuration that leads to the initiation of transcription  
 159 (Fig.5a).

160

161 In our generic model, we consider only a single binding site to which ‘repressor’ and ‘RNAP’  
 162 compete for binding. Note that the model does not make any assumptions about the identity  
 163 of the TFs that are binding DNA and hence does not utilize any specific energy matrix. The  
 164 model is, therefore, general in nature, relying only on the physical and mechanistic  
 165 properties of protein-DNA binding. In such a system, three basic configurations are possible:  
 166 no proteins bound to DNA, only ‘RNAP’ bound, or only ‘repressor’ bound (Fig.5a). Each of  
 167 these states is assigned a Boltzmann weight ( $Z$ ) based on its free binding energy  $E_i$  : 1;  
 168  $[P]e^{-\beta E_P}$ ; and  $[R]e^{-\beta E_R}$ , respectively, where  $\beta$  is  $1/k_B T$ ; subscript  $P$  refers to ‘RNAP’,  
 169 subscript  $R$  to the ‘repressor’;  $[P]$  and  $[R]$  to the exponential of the chemical potential for the  
 170 ‘RNAP’ and the ‘repressor’ which for simplicity we equate to the concentrations of the two  
 171 molecules; and  $E_i$  corresponds to the change in Gibbs free energy of the reaction of the  
 172 binding between protein and DNA. Assuming that the system is in thermodynamic  
 173 equilibrium, we can calculate the probability of finding the system in a configuration leading  
 174 to transcription ( $p_{ON}$ ) – when RNAP is bound:

$$p_{ON} = \frac{[P]e^{-\beta E_P}}{1 + [P]e^{-\beta E_P} + [R]e^{-\beta E_R}}$$

175 The phenotype of a mutant is obtained by calculating  $p_{ON}$  for a free energy  $E'_i = E_i + \Delta$ , where  $\Delta$   
 176 represents the effect of the mutation on the binding of the protein to the sequence. The  
 177 energies of single mutants and double mutants are  $E_P^{m_1} = E_P + p_1$  and  $E_R^{m_1} = E_R + p_1$ ; and  
 178  $E_P^{m_2} = E_P + p_2$  and  $E_R^{m_2} = E_R + p_2$ ; and  $E_P^{m_{12}} = E_P + p_1 + p_2$  and  $E_R^{m_{12}} = E_R + p_1 + p_2$   
 179 ,respectively, where  $p_i$  stands for the effect of mutation  $i$  on the binding of ‘RNAP’ and  $r_i$  for

180 the effect on ‘repressor’ binding. From these measures of the mutational effects, we  
181 calculated epistasis against a multiplicative model, in the same manner as done for the  
182 experimental measurements:

$$p_{ON}^{m_{12}} = \varepsilon p_{ON}^{WT} \frac{p_{ON}^{m_1}}{p_{ON}^{WT}} \frac{p_{ON}^{m_2}}{p_{ON}^{WT}}$$

183

184 With the generic model, we ask only about the sign of epistasis and say that it is positive  
185 when  $\varepsilon > 1$  and negative when  $\varepsilon < 1$ . The generic model cannot predict the magnitude of  
186 epistasis in any particular biological system without accounting for the underlying energy  
187 matrices and intracellular concentrations of relevant TFs. As the model does not account for  
188 the details of any specific regulatory system, it considers only the direct, primary effects of a  
189 mutation on binding affinity ( Bintu et al. 2005a), and does not consider any potential  
190 interactions arising from secondary effects, namely the effects of a mutation on the structure  
191 of DNA (Rajkumar et al. 2013), accessibility to the binding sites (Levo and Segal 2014), protein  
192 cooperativity (Todeschini et al. 2014), looping (Levine et al. 2014), or any other potential  
193 regulatory structures.

194

### 195 **The sign of epistasis can be predicted from first principles**

196 Using the generic model, we first studied the effects of mutations only on ‘RNAP’ binding (in  
197 the absence of ‘repressor’), and found that epistasis depends only on the sign of individual  
198 mutation effects (Fig.5). Our model predicts that if mutations have the same sign, they are  
199 always in negative epistasis. This prediction arises from the non-linear relationship between  
200 binding energy and expression  $p_{on}$  (Fig.5b). Namely, when repressor concentration goes to  
201 zero, epistasis is negative only when  $e^{-p_1} + e^{-p_2} < e^{-p_1-p_2}$  - a condition satisfied only  
202 when  $p_1$  and  $p_2$  have the same sign. Conversely, when the two mutations have a different  
203 sign, they will always be in positive epistasis. In general, the physical properties of the

204 relationship between binding and gene expression indicate that the sign of epistasis for any  
205 given TF depends only on the sign of individual mutation effects ( $p_1$  and  $p_2$ ) upon binding (Fig.  
206 5c).

207

208 Experimental observations do not significantly differ from these predictions for the sign of  
209 epistasis ( $\chi^2_{1,112}=3.64$ ,  $p=0.056$ ), as 96 of the 113 double mutants (85%) that are in significant  
210 epistasis in the absence of CI conform to model predictions. Experimental deviations from  
211 the generic model predictions (i.e., displaying positive epistasis when both mutations have  
212 the same sign) could be due to the secondary effects of mutations, as they could affect the  
213 general context of RNAP binding (Rajkumar et al. 2013), or the ability of CI to bind  
214 cooperatively (Stayrook et al. 2008).

215

216 The model also describes patterns of epistasis in the presence of a repressor. By assuming  
217 that every point mutation affects the binding of both 'RNAP' and 'repressor', we find that the  
218 environmentally dependent change in the sign of epistasis depends on the concentrations of  
219 'RNAP' and 'repressor', as well as the sign and relative magnitude of individual mutation  
220 effects (Table 1 – Source Data 1). At high 'repressor' concentrations, effects of mutations on  
221 'repressor' binding dominate over their effects on 'RNAP binding'. In these environments, the  
222 sign of epistasis depends only on the sign of individual mutation effects on 'repressor'  
223 binding.

224

225 In general, assuming that 'RNAP' concentration stays relatively constant (Raser and O'Shea  
226 2005) allows us to derive how the sign of epistasis depends on repressor concentration  
227 (Table 1). When one point mutation negatively affects only 'RNAP' binding, while the other  
228 only 'repressor' binding (Fig.5d), the system does not exhibit any epistasis when 'repressor'  
229 concentration is very low, as only one of the mutations affects 'RNAP' binding (Fig.5e). As

230 'repressor' concentration increases, the system is in positive epistasis. Finally, at very high  
231 'repressor' concentrations, which are probably not biologically relevant, epistasis approaches  
232 0 as the 'repressor' binds too strongly. When point mutations negatively affect both 'RNAP'  
233 and 'repressor' binding (Fig.5f), epistasis changes the sign from negative to positive as  
234 'repressor' concentration increases (Fig.5g).

235

236 To intuit this finding, consider two mutations that reduce binding of both 'RNAP' and  
237 'repressor'. In the absence of 'repressor', when only 'RNAP' is present, epistasis will be  
238 negative because of the negative curvature of the relationship between expression and  
239 binding energy (Fig.5b). But, in the presence of 'repressor', it is the relative magnitude of  
240 individual mutation effects that will determine the sign of epistasis. This is because mutations  
241 that weaken 'repressor' binding increase expression. If the mutation effects are larger on  
242 'RNAP', then the negative epistasis on expression arising from 'RNAP' will dominate. When  
243 the mutations have a greater effect on 'repressor' binding, then negative epistasis on  
244 'repressor' binding will dominate and lead to positive epistasis on expression, and hence to a  
245 dependence on the environment. At high 'repressor' concentration, only the sign of the  
246 effects of mutations on 'repressor' binding will determine the sign of epistasis. As most  
247 experimentally tested mutations reduce both RNAP and CI binding, our model explains the  
248 observation that most double mutants change the sign of epistasis between the two  
249 environments (Fig.4).

250

### 251 **Independent validation of the generic model predictions**

252 The experimental data from the random mutant library (Fig.3,4) shows that the patterns of  
253 epistasis between two environments follow the generic model predictions, specifically that  
254 epistasis switches sign between environments in many mutants. However, our experimental  
255 design, where we only measure gene expression levels, does not allow us to identify the

256 effects of a mutation on CI binding alone. For example, if a mutation decreases gene  
257 expression level in the presence of CI, we cannot know if it decreases RNAP binding,  
258 increases CI binding, or both. This prevents a more thorough verification of the generic  
259 model. In order to independently experimentally validate the generic model predictions  
260 (Table 1), it is necessary to know the effects of CRE mutations on RNAP and CI. To obtain this  
261 information, we used the experimentally determined energy matrices for RNAP (Kinney et al.  
262 2010) and CI (Sarai and Takeda 1989), and utilized it to create five random double mutants  
263 for each possible combination of single mutation effects shown in Table 1. Due to the high  
264 specificity of binding of both RNAP and CI, we could not identify point mutations that  
265 simultaneously improved the binding of both (Supplementary File 3). Therefore, we validate  
266 the model by measuring epistasis in 30 double mutants (five for each of the six possible  
267 combinations of single mutant effects) in the two environments. We find no difference  
268 between the predicted and experimental estimates of the sign of epistasis and its  
269 dependence on the two experimental environments (Pearson's  $\chi^2_{2,30}=0.68$ ;  $p=0.72$ ) (Fig.6). As  
270 such, the predictions about the sign of epistasis that arise from the generic model (Table 1)  
271 hold true in our experimental system.

272

273 Furthermore, we tested if a simple thermodynamic model that incorporates the two energy  
274 matrices (Sarai and Takeda 1989; Kinney et al. 2010) can predict not only the sign, but also  
275 the magnitude of epistasis in the two environments. Because such a model depends on the  
276 concentrations of RNAP and CI, we estimated the values for these parameters so as to  
277 maximize the correlation between model predictions and empirical values of epistasis. When  
278 we excluded those double mutants which did not empirically exhibit significant epistasis, we  
279 found a significant fit between experimental measurements and model predictions of the  
280 magnitude of epistasis in the absence ( $F_{1,15}=9.86$ ;  $P<0.01$ ) and in the presence of CI  
281 ( $F_{1,15}=4.59$ ;  $P<0.05$ ) (Fig.6 - Figure Supplement 1). As such, the model predicts not only the

282 general patterns of epistasis (sign), but is also reasonably accurate at predicting its  
283 magnitude, which is remarkable since the model does not consider detailed molecular  
284 aspects of the experimental system, such as CI dimerization or cooperativity.

285

## 286 DISCUSSION

287 The theory we present here, which is based on mechanistic properties of protein-DNA  
288 binding without accounting for any details of the molecular system studied, provides an  
289 accurate prediction of the sign of epistasis and its environmental dependence for a  
290 repressible promoter system - the most common form of gene regulation in *E.coli* (~40% of  
291 all regulated genes (Salgado et al. 2013)). Furthermore, the fact that we use a generic model  
292 with no reference to any particular empirical measures means that our results are derived  
293 from first principles. As such, the presented results should hold as long as the effects of  
294 mutations on gene expression are mainly driven by their direct impact on TF-DNA binding, as  
295 represented by the energy matrix for a given TF. Under such conditions, the thermodynamic  
296 model, rather than the multiplicative (or additive) expectation, provides a meaningful null  
297 model for the sign of epistasis in CREs.

298

299 The sign of the deviations from a multiplicative expectation can have important evolutionary  
300 consequences, such as for the evolution of sex (Otto and Lenormand 2002) or the  
301 maintenance of genetic variation (Charlesworth et al. 1995). A particularly important pattern  
302 of epistasis is sign epistasis, where the sign of the effect of a particular substitution depends  
303 on the genetic background. Sign epistasis can lead to the existence of multiple optima (local  
304 peaks). In the system we analyze here, sign epistasis cannot exist in the absence of a  
305 repressor, since there is an optimum binding site sequence and the effects of mutations have  
306 a definite sign towards this optimal sequence. In the presence of a repressor, however, sign  
307 epistasis is possible (Poelwijk et al. 2011). Furthermore, we show that the sign of epistasis



308 very often reverses between environments. This phenomenon, previously observed in a  
309 different system (de Vos et al. 2013; Lagator et al. 2015), could alleviate constraints coming  
310 from the existence of multiple peaks in a particular environment. The thermodynamic model  
311 provides a mechanistic basis for this observation: RNAP and repressor have opposite effects  
312 on gene expression and this, when combined with the specific shape of response induced by  
313 the thermodynamic model, can lead to the environmental dependence of the sign of  
314 epistasis.

315

316 Our results concern the combined effect of mutations (epistasis) on phenotype, as opposed  
317 to fitness. Phenotypes logically precede fitness and even though it could be argued that  
318 fitness is “what matters” for evolution, since mutations spread in part based on their fitness  
319 effects, determining the fitness effects of mutations depends on the environment which may  
320 or may not be representative of “natural” conditions. Moreover, knowledge about one  
321 environment is hardly informative about the fitness patterns in a novel environment. Our  
322 results allow for the prediction of patterns of phenotypic epistasis across different  
323 environmental conditions, independent of the selection pressures applied to this phenotype.  
324 The evolutionary consequences of these patterns of epistasis can then be inferred from the  
325 knowledge (or assumptions) of how selection is acting on this phenotype, or in other words,  
326 how the phenotype maps onto fitness.

327

328 In order to predict the sign of epistasis in a regulatory system, the thermodynamic model  
329 accounts for the underlying physical mechanisms that impose constraints on the genotype-  
330 phenotype map under consideration. Incorporating details of physical and molecular  
331 mechanisms into models of more complex regulatory elements, as well as coding sequences  
332 (Dean and Thornton 2007; Li et al. 2016), can elucidate how epistasis impacts genotype-

333 phenotype maps and their dynamic properties across environments, helping us to  
334 understand the environmental dependence of fitness landscapes.

335

336 MATERIALS AND METHODS

### 337 **Gene regulation in the $P_R$ promoter system**

338 We developed a system based on the *right* regulatory element of the lambda phage ( $P_R$ ), in  
339 which we decoupled the *cis*- and *trans*-regulatory elements (Fig.2) (Johnson et al. 1981). A  
340 *Venus-yfp* gene (Nagai et al. 2002) is placed under the control of the *cis*-regulatory region  
341 containing the  $P_R$  promoter with two lambda repressor CI binding sites ( $O_{R1}$  and  $O_{R2}$ ). The  
342 transcription factor CI represses the  $P_R$  promoter by direct binding-site competition with  
343 RNAP. Separated by 500 random base pairs and on the opposite DNA strand, we placed the *ci*  
344 repressor gene under the control of a  $P_{TET}$  promoter (Lutz and Bujard 1997), followed by a  
345 TL17 terminator sequence. Thus, concentration of CI transcription factor in the cell was  
346 under external control, achieved by addition of the inducer anhydrotetracycline (aTc). The  
347 entire cassette was inserted into the low-copy number plasmid pZS\* carrying kanamycin  
348 resistance gene (Lutz and Bujard 1997).

349

### 350 **Random mutant library**

351 We created a library of random single and double mutants in the 43bp *cis*-regulatory element  
352 (consisting of the RNAP binding site and the two CI operator sites  $O_{R1}$  and  $O_{R2}$ ) using the  
353 GeneMorph II™ random mutagenesis kit (Agilent Technologies, Santa Clara, US). PCR  
354 products of mutagenesis reactions were ligated into the wildtype plasmid and inserted into a  
355 modified *Escherichia coli* K12 strain MG1655 chromosomally expressing *tetR* gene from a  
356  $PN_{25}$  promoter. We sequenced ~500 colonies in order to create a library of 141 double  
357 mutants for which both corresponding single mutants were also identified (Supplementary  
358 File 1). We identified, in total, 89 mutants carrying only a single point mutation. Four single

359 and four double mutants from the library were randomly selected and the whole plasmid  
360 sequenced to confirm that during library construction no mutations were found outside the  
361 target regulatory region.

362

363 We measured fluorescence for each single and double mutant, as well as the wildtype  $P_R$   
364 promoter system, both in the presence and in the absence of the inducer aTc. Six replicates  
365 of each mutant in the library were grown overnight in M9 media, supplemented with 0.1%  
366 casamino acids, 0.2% glucose, 30 $\mu$ g/ml kanamycin, either without or with 15ng/ml aTc.  
367 Presence or absence of aTc determined the two experimental environments. Overnight  
368 cultures were diluted 1,000X, grown to OD<sub>600</sub> of approximately 0.05, and their fluorescence  
369 measured in Bio-Tek Synergy H1 platereader. The measured fluorescence was first corrected  
370 for the autofluorescence of the media, and then normalized by the wildtype fluorescence. All  
371 replicate measurements were randomized across multiple 96-well plates. All replicates were  
372 biological, having been kept separate from each other from the moment that the mutant was  
373 cloned and identified through sequencing. Six replicates of each mutant were measured as  
374 prior experience with similar datasets in the lab has shown it sufficient to detect meaningful  
375 differences between mutants.

376

### 377 **Statistical analyses**

378 By using a multiplicative model of epistasis, we calculated epistasis relative to the wildtype as  
379  $\epsilon = f_{m_{12}} / (f_{m_1}f_{m_2})$ , where  $f_{m_{12}}$  is the relative fluorescence of a double mutant ( $m_{12}$ ), and  $f_{m_1}$  and  
380  $f_{m_2}$  the relative fluorescence of the two corresponding single mutants ( $m_1$  and  $m_2$ ),  
381 respectively. In order to determine statistically which double mutants exhibit epistasis (i.e.  $\epsilon$   
382 not equal 1), we conducted a series of FDR-corrected  $t$ -tests. The errors were calculated  
383 based on six replicates, using error propagation to account for the variance due to  
384 normalization by the wildtype. Variance is not significantly different between measured

385 mutants (Figure 3 – Figure supplement 1; Figure 3 – Figure supplement 2). We performed a  
386 Pearson’s *chi*-squared test to determine if double mutants had a tendency towards negative  
387 epistasis. We asked whether epistasis depended on the environment (defined as presence or  
388 absence of the repressor) by testing for a genotype x genotype x environment (GxGxE)  
389 interaction using ANOVA. We also tested if the experimental observations of the sign of  
390 epistasis in the absence of CI repressor corresponded to model predictions. To do that, we  
391 used the experimental measurements of the sign of single mutation effects to predict the  
392 sign of epistasis (if both mutations had the same sign then epistasis was predicted to be  
393 negative, if they differed in sign, it was predicted as positive). Then we compared the  
394 predicted distribution of the sign of epistasis to the experimental estimates using a *chi*-  
395 squared test, limiting the test to only those double mutants that experimentally exhibited  
396 significant epistasis. For all tests, data met the assumptions, and variance between groups  
397 was not significantly different.

398

#### 399 **Generic model of gene regulation with binding site competition between RNAP and** 400 **repressor**

401 The model is based on previous thermodynamic approaches (Bintu et al. 2005a,b; Hermsen  
402 et al. 2006). These models consider all possible promoter occupancy states and assign a  
403 Boltzmann weight to each state. The probability of any microstate (promoter configurations)  
404 is given by Boltzmann weights  $w_i = e^{-\beta E_i - N\mu}$ , where  $E_i$  is the Gibbs free energy of the  
405 configuration,  $N$  is the number of TF molecules,  $\beta$  is  $1/k_B T$ , and  $\mu$  represents the chemical  
406 potential.  $p_{on}$  can then be calculated as the normalized sum of all configurations conducive to  
407 the initiation of transcription:

$$p_{ON} = \frac{\sum_{i \in \Phi} w_i}{\sum_i w_i}$$

408 Where the first summation is over the all configurations conducive to transcription, whereas  
 409 the second is over all configurations.

410

411 In our model, we consider a scenario in which an activator (such as RNAP) competes with a  
 412 repressor for access to its binding site. We consider only three possible promoter  
 413 configurations: the one where neither of the two proteins is bound, the one in which a  
 414 ‘repressor’ prevents ‘RNAP’ from accessing its binding site, and the one in which ‘RNAP’ is  
 415 bound to its binding site, thereby able to initiate transcription. Under these assumptions, the  
 416 probability of initiation of transcription is:

$$p_{ON} = \frac{[P]e^{-\beta E_P}}{1 + [P]e^{-\beta E_P} + [R]e^{-\beta E_R}}$$

417 where  $[P]$  and  $[R]$  represent the exponential of the chemical potential for the ‘RNAP’ and the  
 418 ‘repressor’, respectively; and subscripts  $P$  and  $R$  represent ‘RNAP’ and ‘repressor’,  
 419 respectively. Throughout, we measure free energies in natural units such that  $\beta=1$ .

420

421 We assume that mutations simultaneously affect the binding of both ‘RNAP’ and ‘repressor’  
 422 to the DNA binding site. We denote the free energies of both ‘RNAP’ and ‘repressor’ binding  
 423 to DNA by  $E_P$  and  $E_R$ , respectively. We model the effect of mutations by perturbing these  
 424 energies by an additive factor. The energies of single mutants and double mutants are then  
 425  $E_P^{m_1} = E_P + p_1$  and  $E_R^{m_1} = E_R + p_1$  ; and  $E_P^{m_2} = E_P + p_2$  and  $E_R^{m_2} = E_R + p_2$  ; and  
 426  $E_P^{m_{12}} = E_P + p_1 + p_2$  and  $E_R^{m_{12}} = E_R + p_1 + p_2$  ,respectively,

427

428 We calculate epistasis against a multiplicative model for the effect of mutations on  $p_{ON}$ :

$$p_{ON}^{m_{12}} = \epsilon p_{ON}^{WT} \frac{p_{ON}^{m_1}}{p_{ON}^{WT}} \frac{p_{ON}^{m_2}}{p_{ON}^{WT}}$$

429 and so epistasis is measured by:

$$\varepsilon = \frac{p_{ON}^{WT} p_{ON}^{m_{12}}}{p_{ON}^{m_1} p_{ON}^{m_2}} = \frac{(1 + Ae^{-r_1} + Be^{-p_1})(1 + Ae^{-r_2} + Be^{-p_2})}{(1 + A + B)(1 + Ae^{-r_1-r_2} + Be^{-p_1-p_2})}$$

430 where  $A = [R]e^{-E_R}$  and  $A = [P]e^{-E_P}$ . We say that epistasis is positive when  $\varepsilon > 1$  and  
 431 negative when  $\varepsilon < 1$ . We then find the conditions for which epistasis is positive in the presence  
 432 ( $A > 0$ ) or absence ( $A = 0$ ) of repressor.

433

#### 434 **Empirical verification of the generic model**

435 In order to empirically test the predictions of the generic model on the relationship between  
 436 sign of individual mutations and the sign of epistasis in two environments, we aimed to select  
 437 5 random double mutants from each category from Table 1. Effects of mutations on RNAP  
 438 and on CI were obtained from the experimentally determined energy matrices of RNAP  
 439 (Kinney et al. 2010) and CI (Sarai and Takeda 1989) binding. We could not validate the model  
 440 from the random mutant library, as the majority of mutants fell in regions that are poorly  
 441 described by the energy matrices. For this reason, we aimed to create this new library. As the  
 442  $P_R$  promoter is very strong, finding double mutants where both mutations improved  
 443 expression was not possible. Hence, we selected 5 double mutants from 6 categories  
 444 (Supplementary File 3), and synthesized them, as well as their corresponding single mutants,  
 445 using annealed oligonucleotide overlap cloning. We measured fluorescence of these mutants  
 446 and calculated epistasis in the same manner as described for the random mutant library, and  
 447 we asked if the epistasis for each double mutant was different from the null-expectation in  
 448 the manner described in section ‘Statistical analyses’. We used Pearson’s *chi*-square test to  
 449 determine if the environmental-dependence of the sign of epistasis in the experimental  
 450 measurements differs from model predictions.

451

452 In order to test whether the thermodynamic model can also predict the magnitude of  
 453 epistasis, we incorporated the energy matrices for RNAP (Kinney et al. 2010) and CI (Sarai

454 and Takeda 1989) into the generic model. As the energy matrix for RNAP contained one  
455 additional position in the spacer region between -10 and -35 sites compared to the  
456 experimental P<sub>R</sub> system, we eliminated one position in that region that had lowest impact on  
457 overall RNAP binding. In the manner described above, we modeled epistasis in those mutants  
458 from the 30-mutant validation library that exhibited significant epistasis. As the  
459 thermodynamic model depends on the concentrations of RNAP and CI, we estimated the  
460 values for these parameters so as to maximize the correlation between model predictions  
461 and empirical values of epistasis. In order to estimate how well the model predicted the  
462 magnitude of epistasis, we fitted a linear regression between experimental measurements of  
463 epistasis and the model predictions, both in the absence and in the presence of CI.

464

#### 465 **Acknowledgments**

466 We thank H. Acar, S. Sarikas, and G. Tkacik for discussion and useful comments on the  
467 manuscript. This work was supported by the People Programme (Marie Curie Actions) of the  
468 European Union's Seventh Framework Programme (FP7/2007-2013) under REA grant  
469 agreement n° [291734] to M.L., has received funding from the European Union's Seventh  
470 Framework Programme for research, technological development and demonstration under  
471 grant agreement no 618091 (SAGE) to T.P. and European Research Council under the Horizon  
472 2020 Framework Programme (FP/2007-2013) / ERC Grant Agreement n. [648440] to J.P.B.

473

#### 474 **Competing interests**

475 The authors declare no competing financial or non-financial interests.

476

#### 477 **Supplementary data files**

478 "Supplementary file 1" – Identity of randomly generated double mutants

479 "Supplementary file 2" – Types of epistasis in two environments

480 “Supplementary file 3” – Identity of mutants used for verification of the model

481

482 REFERENCES

483 Ackers, G. K., A. D. Johnson, and M. A. Shea. 1982. Quantitative Model for Gene Regulation  
484 by Lambda Phage Repressor. *PNAS* 79:1129–1133.

485 Bintu, L., N. E. Buchler, H. G. Garcia, U. Gerland, T. Hwa, J. Kondev, and R. Phillips. 2005a.  
486 Transcriptional Regulation by the Numbers: Models. *Current Opinion in Genetics &*  
487 *Development* 15:116–124.

488 Bintu, L., N. E. Buchler, H. G. Garcia, U. Gerland, T. Hwa, J. Kondev, T. Kuhlman, and R.  
489 Phillips. 2005b. Transcriptional Regulation by the Numbers: Applications. *Current Opinion in*  
490 *Genetics & Development* 15:125–135.

491 Breen, M. S., C. Kemena, P. K. Vlasov, C. Notredame, and F. A. Kondrashov. 2012. Epistasis as  
492 the Primary Factor in Molecular Evolution. *PNAS* 109:535–538.

493 Caudle, S. B., C. R. Miller, and D. R. Rokytka. 2014. Environment Determines Epistatic Patterns  
494 for a ssDNA Virus. *Genetics* 196:267–279.

495 Charlesworth, D., B. Charlesworth, and M. T. Morgan. 1995. The Pattern of Neutral  
496 Molecular Variation Under the Background Selection Model. *Genetics* 141:1619–1632.

497 Cordell, H. J. 2002. Epistasis: What it Means, What it Doesn’t Mean, and Statistical Methods  
498 to Detect it in Humans. *Human Molecular Genetics* 11:2463–2468.

499 de Visser, J. A. G. M., and J. Krug. 2014. Empirical Fitness Landscapes and the Predictability  
500 of Evolution. *Nature Reviews Genetics* 15:480–490.

501 de Vos, M., F. J. Poelwijk, N. Battich, J. D. T. Ndika, and S. J. Tans. 2013. Environmental  
502 Dependence of Genetic Constraint. *PLoS Genetics* 9:e1003580.

503 Dean, A. M., and J. W. Thornton. 2007. Mechanistic Approaches to the Study of Evolution:  
504 the Functional Synthesis. *Nature Reviews Genetics* 8:675–688.

505 Dettman, J. R., C. Sirjusingh, L. M. Kohn, and J. B. Anderson. 2007. Incipient Speciation by  
506 Divergent Adaptation and Antagonistic Epistasis in Yeast. *PNAS* 104:585–588.

507 Flynn, K. M., T. F. Cooper, F. B.-G. Moore, and V. S. Cooper. 2013. The Environment Affects  
508 Epistatic Interactions to Alter the Topology of an Empirical Fitness Landscape. *PLoS Genetics*  
509 9:e1003426.

510 Garcia, H. G., A. Sanchez, J. Q. Boedicker, M. Osborne, J. Gelles, J. Kondev, and R. Phillips.  
511 2012. Operator Sequence Alters Gene Expression Independently of Transcription Factor  
512 Occupancy in Bacteria. *Cell Reports* 2:150–161.

513 Hermsen, R., S. Tans, and P. R. ten Wolde. 2006. Transcriptional regulation by competing  
514 transcription factor modules. *PLoS computational biology* 2:e164.

515 Johnson, A. D., A. R. Poteete, G. Lauer, R. T. Sauer, G. K. Ackers, and M. Ptashne. 1981.  $\lambda$



- 516 Repressor and *cro* - components of an Efficient Molecular Switch. 294:217–223.
- 517 Kinney, J. B., A. Murugan, C. G. J. Callan, and E. C. Cox. 2010. Using Deep Sequencing to  
518 Characterize the Biophysical Mechanism of a Transcriptional Regulatory Sequence. PNAS  
519 107:9158–9163.
- 520 Kondrashov, A. S. 1988. Deleterious mutations and the evolution of sexual reproduction.  
521 336:435–440.
- 522 Kondrashov, D. A., and F. A. Kondrashov. 2014. Topological Features of Rugged Fitness  
523 Landscapes in Sequence Space. Trends in Genetics TIGS–1156.
- 524 Kussell, E. 2013. Evolution in Microbes. Annu. Rev. Biophys. 42:493–514.
- 525 Lagator, M., C. Igler, A. B. Moreno, C. C. Guet, and J. P. Bollback. 2015. Epistatic Interactions  
526 in the Arabinose *cis* Regulatory Element. Molecular Biology and Evolution msv269–12.
- 527 Lalic, J., and S. F. Elena. 2012. Epistasis between Mutations is Host-Dependent for an RNA  
528 Virus. Biol Lett 9:20120396.
- 529 Lehner, B. 2013. Genotype to Phenotype: Lessons from Model Organisms for Human  
530 Genetics. Nature Reviews Genetics 14:168–178.
- 531 Lehner, B. 2011. Molecular Mechanisms of Epistasis within and between Genes. Trends in  
532 Genetics 27:323–331.
- 533 Levine, M., C. Cattoglio, and R. Tjian. 2014. Looping Back to Leap Forward: Transcription  
534 Enters a New Era. Cell 157:13–25.
- 535 Levo, M., and E. Segal. 2014. In Pursuit of Design Principles of Regulatory Sequences. Nature  
536 Reviews Genetics 15:453–468.
- 537 Li, C., W. Qian, C. Maclean, and J. Zhang. 2016. The Fitness Landscape of a tRNA Gene.  
538 Science 352:837–840.
- 539 Lutz, R., and H. Bujard. 1997. Independent and Tight Regulation of Transcriptional Units in  
540 *Escherichia coli* via the LacR/O, the TetR/O and AraC/I1-I2 Regulatory Elements. Nucleic  
541 Acids Research 25:1203–1210.
- 542 Maerkl, S. J., and S. R. Quake. 2009. Experimental Determination of the Evolvability of a  
543 Transcription Factor. Proceedings of the National Academy of Sciences 106:18650–18655.
- 544 Nagai, T., K. Ibata, E. S. Park, M. Kubota, K. Mikoshiba, and A. Miyawaki. 2002. A Variant of  
545 Yellow Fluorescent Protein with Fast and Efficient Maturation for Cell-Biological  
546 Applications. Nature Biotechnology 20:87–90.
- 547 Orr, A. H., and M. Turelli. 2001. The Evolution of Postzygotic Isolation: Accumulating  
548 Dobzhansky-Muller Incompatibilities. Evolution 55:1085–1094.
- 549 Otto, S. P., and T. Lenormand. 2002. Resolving the paradox of sex and recombination. Nature  
550 Reviews Genetics 3:252–261.
- 551 Phillips, P. C. 2008. Epistasis — the Essential Role of Gene Interactions in the Structure and

- 552 Evolution of Genetic Systems. *Nature Reviews Genetics* 9:855–867.
- 553 Poelwijk, F. J., S. Tănase-Nicola, D. J. Kiviet, and S. J. Tans. 2011. Reciprocal Sign Epistasis is a  
554 Necessary Condition for multi-Peaked Fitness Landscapes. *Journal of Theoretical Biology*  
555 272:141–144.
- 556 Ptashne, M. 2011. Principles of a Switch. *Nat Chem Biol* 7:484–487.
- 557 Rajkumar, A. S., N. Déneraud, and S. J. Maerkl. 2013. Mapping the Fine Structure of a  
558 Eukaryotic Promoter Input-Output Function. *Nature Genetics* 45:1207–1215.
- 559 Raser, J. M., and E. K. O'Shea. 2005. Noise in Gene Expression: Origins, Consequences, and  
560 Control. *Science* 309:2010–2013.
- 561 Sackton, T. B., and D. L. Hartl. 2016. Genotypic Context and Epistasis in Individuals and  
562 Populations. *Cell* 166:279–287.
- 563 Saiz, L., and J. M. G. Vilar. 2008. Ab initio Thermodynamic Modeling of Distal Multisite  
564 Transcription Regulation. *Nucleic Acids Research* 36:726–731.
- 565 Salgado, H., M. Peralta-Gil, S. Gama-Castro, A. Santos-Zavaleta, L. Muñiz-Rascado, J. S.  
566 García-Sotelo, V. Weiss, H. Solano-Lira, I. Martínez-Flores, A. Medina-Rivera, G. Salgado-  
567 Osorio, S. Alquicira-Hernández, K. Alquicira-Hernández, A. López-Fuentes, L. Porrón-Sotelo,  
568 A. M. Huerta, C. Bonavides-Martínez, Y. I. Balderas-Martínez, L. Pannier, M. Olvera, A.  
569 Labastida, V. Jiménez-Jacinto, L. Vega-Alvarado, V. Del Moral-Chávez, A. Hernández-Alvarez,  
570 E. Morett, and J. Collado-Vides. 2013. RegulonDB v8.0: Omics Data Sets, Evolutionary  
571 Conservation, Regulatory Phrases, Cross-Validated Gold Standards and More. *Nucleic Acids*  
572 *Research* 41:D203–13.
- 573 Sarai, A., and Y. Takeda. 1989. Lambda Repressor Recognizes the Approximately 2-fold  
574 Symmetric Half-Operator Sequences Asymmetrically. *PNAS* 86:6513–6517.
- 575 Schuster, P. 2006. Prediction of RNA Secondary Structures: from Theory to Models and Real  
576 Molecules. *Rep. Prog. Phys.* 69:1419–1477.
- 577 Shultzaberger, R. K., S. J. Maerkl, J. F. Kirsch, and M. B. Eisen. 2012. Probing the  
578 Informational and Regulatory Plasticity of a Transcription Factor DNA-Binding Domain. *PLoS*  
579 *Genetics* 8:e1002614.
- 580 Starr, T. N., and J. W. Thornton. 2016. Epistasis in Protein Evolution. *Protein Sci.* 25:1204–  
581 1218.
- 582 Stayrook, S., P. Jaru-Ampornpan, J. Ni, A. Hochschild, and M. Lewis. 2008. Crystal structure of  
583 the  $\lambda$  repressor and a model for pairwise cooperative operator binding. 452:1022–1025.
- 584 Szathmáry, E. 1993. Do Deleterious Mutations Act Synergistically? *Metabolic Control Theory*  
585 Provides a Partial Answer. *Genetics* 133:127–132.
- 586 Szendro, I. G., J. Franke, J. A. G. de Visser, and J. Krug. 2013. Predictability of Evolution  
587 depends Nonmonotonically on Population Size. *PNAS* 110:571–576.
- 588 Todeschini, A.-L., A. Georges, and R. A. Veitia. 2014. Transcription Factors: Specific DNA  
589 Binding and Specific Gene Regulation. *Trends in Genetics* 30:211–219.

590 Valenich, A., and J. Gore. 2013. The Strength of Genetic Interactions Scales Weakly with  
 591 Mutational Effects. *Genome Biol* 14:R76.

592 Vilar, J. M. G. 2010. Accurate Prediction of Gene Expression by Integration of DNA Sequence  
 593 Statistics with Detailed Modeling of Transcription Regulation. *Biophysical Journal* 99:2408–  
 594 2413.

595 Weinreich, D. M., N. F. Delaney, M. A. DePristo, and D. Hartl. 2006. Darwinian Evolution Can  
 596 Follow Only Very Few Mutational Paths to Fitter Proteins. *Science* 312:111–114.

597 Wolf, J. B., E. D. Brodie, and M. J. Wade. 2000. *Epistasis and the Evolutionary Process*. Oxford  
 598 University Press, Oxford, UK.

599 Woods, R. J., J. E. Barrick, T. F. Cooper, U. Shrestha, M. R. Kauth, and R. E. Lenski. 2011.  
 600 Second-order selection for evolvability in a large *Escherichia coli* population. *Science*  
 601 331:1433–1436.

602

603

604 FIGURES AND TABLES

605 **TABLE 1.**

606

		$p_1 r_1$			
		- -	+ -	- +	+ +
$p_2 r_2$	+ +	pos → neg neg → pos	neg → pos	pos → neg	neg → pos
	- +	pos → neg	always positive	always negative	
	+ -	pos → neg	always negative		
	- -	neg → pos			

607

608 **Table 1: Sign of epistasis in a simple CRE depends on the environment and the sign of**

609 **individual mutation effects.** We consider two environments, one without repressor when

610 mutations affect only RNAP binding, and the other with high repressor concentration. In the

611 first environment, sign of epistasis is determined only by the sign of individual mutation

612 effects on RNAP binding, while in the second environment it is the sign of individual

613 mutation effect on the repressor that matters. For each mutation, the signs ('+' and '-')

614 represent the sign of its effect on the binding of RNAP ( $p$ ) and repressor ( $r$ ), respectively.

615 'neg → pos' and 'pos → neg' represent combinations that display transitions from negative

616 to positive, or positive to negative epistasis, respectively. Certain combinations of mutations  
617 are always in negative or always in positive epistasis. The extended version of this table,  
618 which does not assume a constant 'RNAP' concentration in the cell, is provided in Table 1 –  
619 Source Data 1.

620

621

622 **Figure 1. The different types of epistasis between two point mutations.** Two point  
623 mutations, A and B (grey), individually increase the measured quantitative phenotype (gene  
624 expression, for example) compared to the wildtype. In this study, we use the multiplicative  
625 expectation of how the phenotypic effects of two mutations contribute to the double mutant  
626 phenotype, according to which  $\text{epistasis} = f_{m_{12}} / (f_{m_1}f_{m_2})$ , where  $f_{m_{12}}$  is the relative  
627 fluorescence of a double mutant ( $m_{12}$ ), and  $f_{m_1}$  and  $f_{m_2}$  the relative fluorescence of the two  
628 corresponding single mutants ( $m_1$  and  $m_2$ ), respectively. An alternative to the multiplicative  
629 assumption would be the additive one, in which the effect of the double mutant in the  
630 absence of epistasis is the sum of the effects of single mutants. The multiplicative model is a  
631 better assumption for gene expression data, as there is a lower limit on this trait (Cordell  
632 2002). In the absence of an interaction between mutations ('no epistasis' scenario,  
633 represented by a grey circle) the phenotype of the double mutant is the product of the  
634 individual mutation. If the effect of the double mutant is greater or lower than the  
635 multiplicative expectation, the two mutations are said to be in positive (blue) or negative  
636 (orange) magnitude epistasis, respectively. Sign epistasis (dark green) occurs when one  
637 mutation has the opposite effect in the presence of the other (as for mutation B above).  
638 Reciprocal sign epistasis (light green) indicates a situation when both mutations have the  
639 opposite effect when in the presence of the other, compared to when they occur  
640 independently on the wildtype background.

641

642 **Figure 2. Experimental system.** The  $P_R$  promoter system used in the empirical measurements  
643 consists of a strong lambda phage  $P_R$  promoter (RNAP binding site) and two CI operator sites  
644 (transcription factor binding sites  $O_{R1}$  and  $O_{R2}$ ), which control the expression of a *venus-yfp*  
645 reporter gene. *ci* is encoded on the opposite strand, separated by a terminator and 500bp of  
646 random sequence, and under the control of an inducible promoter  $P_{TET}$ . Both *venus-yfp* and *ci*  
647 genes are followed by a terminator sequence. a) In the absence of CI, the promoter is fully  
648 expressed. b) CI binds cooperatively to two operators in order to repress the promoter.

649

650

651 **Figure 3. Epistasis in the absence and in the presence of CI.** Points show  $\log_{10}$  of expected  
652 versus  $\log_{10}$  of observed double mutant effects (each relative to wildtype fluorescence) for all  
653 141 double mutants, in the **a)** absence; and **b)** presence of the CI repressor. The solid line  
654 represents no epistasis (expected equal to the observed double mutant expression). Six  
655 replicates of each mutant were measured. Bar charts show total number of double mutants  
656 exhibiting positive (orange) and negative (blue) epistasis, while the darker areas represent  
657 the number that are significantly different from the null expectation of the model (no  
658 epistasis). The data presented in this figure can be found in Fig.3 – Figure Supplement 1, Fig.3  
659 – Figure Supplement 2, and Figure 3 – Source Data 1.

660

661

662 **Figure 4. Sign of epistasis changes with the environment for most double mutants.** Points  
663 show the  $\log_{10}$  value of epistasis in the absence of repressor, and the difference in the  $\log_{10}$   
664 value of epistasis in the presence and the absence of repressor -  $\log_{10}(\epsilon_{CI}) - \log_{10}(\epsilon_{noCI})$ , for all  
665 141 double mutants. Points above the solid diagonal line exhibit positive, while points below  
666 exhibit negative epistasis in the presence of the CI repressor. Most mutants have a different  
667 sign of epistasis between the two environments (gray area). Bar chart shows total number of

668 double mutants that are always in positive (orange) or in negative (blue) epistasis, and the  
669 total number that changes sign between the two environments (gray). The darker areas in  
670 the bars represent the number that are significantly different from the null expectation of  
671 the model (no epistasis) in both environments. Six replicates of each mutant were measured.  
672 The data presented in this figure is calculated from Figure 3 – Source Data 1.

673

674

675 **Figure 5. Overview of the generic model.** The theoretical approach used in this study,  
676 originally developed to describe gene regulation by the lambda bacteriophage repressor CI  
677 (Ackers et al. 1982), relies on statistical thermodynamics assumptions to model initiation of  
678 transcription. **a)** In this framework, each DNA-binding protein is assigned a binding energy ( $E_i$ )  
679 to an arbitrary stretch of DNA. Given a set of DNA binding proteins (a generic RNAP-like and a  
680 generic repressor-like TF, in this case) and a promoter sequence, a Boltzmann weight can be  
681 assigned to any configuration of these TFs on the promoter. By assigning a Boltzmann weight  
682 to all configurations, one can calculate the probability of finding the system in a configuration  
683 that leads to the initiation of transcription. **b)** When considering only the binding of a single  
684 protein to DNA (for example 'RNAP' only), if mutations have a negative effect on protein-DNA  
685 binding, the model predicts negative epistasis between them in terms of expression. This  
686 prediction arises from the non-linear relationship between binding energy and gene  
687 expression  $p_{on}$  (dotted line). In this illustration, we show a relative change in binding energy  
688 compared to the sequence with highest possible binding, in kT. **c)** By generalizing the  
689 properties of the relationship between binding and gene expression, we conclude that the  
690 sign of epistasis depends only on the sign of individual mutation effects ( $p_1$  and  $p_2$ ) upon  
691 binding. When both 'RNAP' and 'repressor' are present in the system, epistasis depends on  
692 the 'repressor' concentration and the magnitude of single mutation effects on 'RNAP' and  
693 'repressor' binding (**d,e,f,g**). **d)** One point mutation negatively affects only 'RNAP' binding,

694 while the other only 'repressor' binding. **e)** Under such circumstances, the system shows no  
695 epistasis at low 'repressor' concentrations, but is in positive epistasis when 'repressor'  
696 concentration increases. Finally, at very high repressor concentrations, epistasis approaches  
697 0. **f)** Point mutations negatively affect both 'RNAP' and 'repressor' binding. **g)** Under such  
698 conditions, epistasis changes the sign from negative to positive as repressor concentration  
699 increases.

700

701

702 **Figure 6. The thermodynamic model accurately predicts sign of epistasis and its**  
703 **environment-dependence.** In order to conduct an independent test of the assumptions of  
704 the generic model, we expanded the generic model to include specific information about the  
705 two TFs relevant to the experimental system – namely, the energy matrices for RNAP (Kinney  
706 et al. 2010) and CI (Sarai and Takeda 1989). We could not use the 141 random mutants to  
707 validate the model, as most of them contained mutations that were in the regions of the CRE  
708 that were poorly characterized by the energy matrices. Therefore, using the energy matrices,  
709 we had to create a new library consisting of 5 random double mutants for each category  
710 from Table 1. As we could not identify any single point mutations that simultaneously  
711 improved the binding of both RNAP and repressor, we tested if empirical measurements of  
712 epistasis conformed to model predictions in 30 mutants. The model predictions of the sign of  
713 epistasis and its environment dependence were based only on the sign of individual mutation  
714 effects on RNAP and repressor binding. The location of points corresponds to the  
715 experimental measurement of epistasis for each mutant, while the color indicates the model  
716 prediction: (i) blue - double mutants predicted to be in negative epistasis both in the absence  
717 and in the presence of the repressor CI; (ii) orange - double mutants that are always in  
718 positive epistasis; (iii) grey - double mutants predicted to change the sign of epistasis in the  
719 two environments. The color intensity indicates significance – lighter shades represent non-

720 significant, darker shades represent significant epistasis in both environments (see ‘Empirical  
 721 verification of the thermodynamic model’ section in Online Methods). Six replicates of each  
 722 mutant were measured. The data underlying this figure is presented in Figure 6 – Source Data  
 723 1. The quantitative test of how well the thermodynamic model predicts the magnitude of  
 724 epistasis in this dataset is presented in Fig.6 – Figure Supplement 1.

725

726

727 **Table 1 – Source Data 1. General conditions for the sign of epistasis in two environments.**

728 Conditions for positive epistasis on gene expression where  $A = [R]e^{-E_R}$ ,  $B = [P]e^{-E_P}$ ,

729  $A^* = \frac{p_1+p_2-p_1p_2-1}{(p_1-r_1)(p_2-r_2)}$  and  $B^* = \frac{A(r_1+r_2-r_1r_2-1)}{1-p_1-p_2+p_1p_2+A(p_1p_2-p_2r_1-p_1r_2+r_1r_2)}$ . “+” mutation means that

730 it improves the binding of that protein to the binding site, a “-” mutation decreases binding  
 731 affinity.  $r_1$ ,  $p_1$  are the effects ( $r_i, p_i = e^{-\epsilon}$ ) of mutation 1 on the repressor, and the  
 732 polymerase, respectively.

733

734

735 **Figure 3 – Figure Supplement 1. Relative fluorescence of single mutants.** Bars are mean  
 736 fluorescence relative to wildtype in the a) absence; and b) presence of the repressor CI.  
 737 Mean fluorescence shown in ascending order. The dotted line shows the wildtype  
 738 fluorescence. Error bars are standard deviations.

739

740

741 **Figure 3 – Figure Supplement 2. Relative fluorescence of double mutants.** Bars are mean  
 742 fluorescence relative to wildtype in the a) absence; and b) presence of the repressor CI.  
 743 Mean fluorescence shown in ascending order. The dotted line shows the wildtype  
 744 fluorescence. Error bars are standard deviations.

745

746

747 **Figure 3 – Source Data 1. Fluorescence measurements of single and double mutants, and**  
 748 **the calculated values for epistasis for the random mutant library.** Multiplicative epistasis,  
 749 both in the absence and in the presence of the repressor CI, for each double mutant from



750 the random mutant library is provided along with the standard deviation for the  
751 measurement, the t-test value (5 degrees of freedom), and the FDR-corrected P value.  
752 Double mutants that do not exhibit a significant epistatic interaction are marked in green.  
753 Wildtype normalized fluorescence measurement of each single and double mutant, from  
754 which the epistasis values were calculated, is also provided for both environments.

755

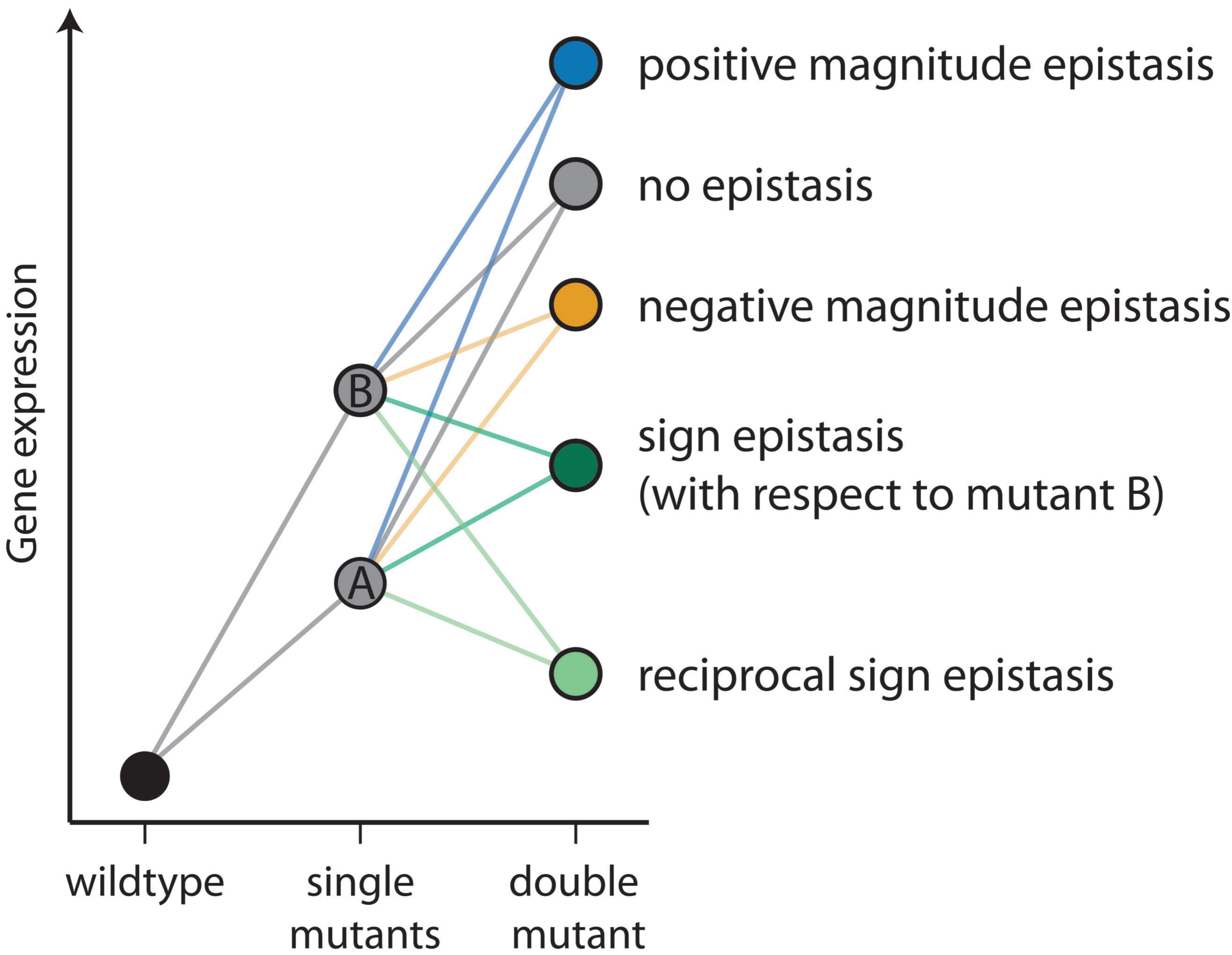
756

757 **Figure 6 – Figure Supplement 1. The thermodynamic model predicts the magnitude of**  
758 **epistasis.** By incorporating specific information about the biological system studied, in the  
759 form of energy matrices for RNAP (Kinney et al. 2010) and CI (Sarai and Takeda 1989), we  
760 could test if the model predicts not only the sign, but also the magnitude of epistasis. Linear  
761 regression between empirical measurements and the model predictions of epistasis is  
762 shown (dashed line) for all mutants in Figure 5 that exhibited significant epistasis. Epistasis  
763 was estimated in the **a)** absence; and **b)** presence of CI. Grey lines show no epistasis  
764 (epistasis value of 1).

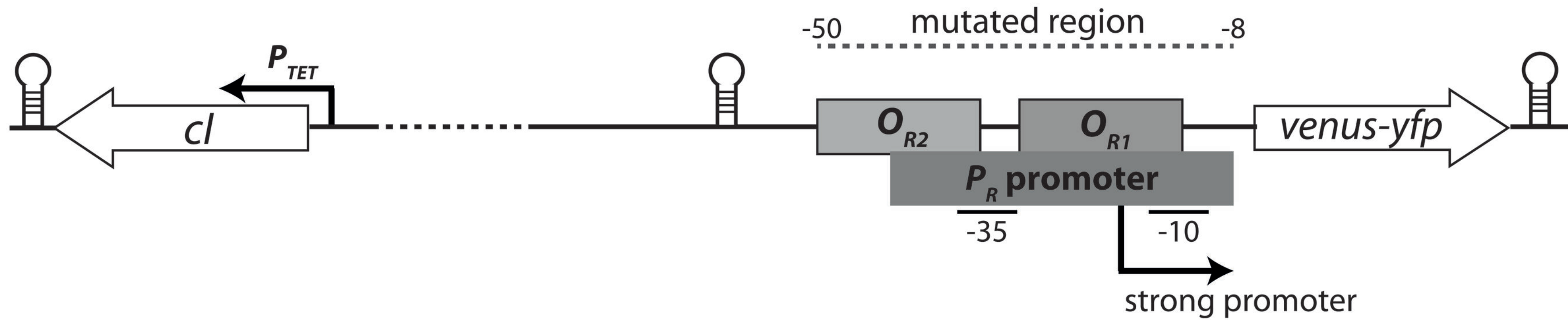
765

766

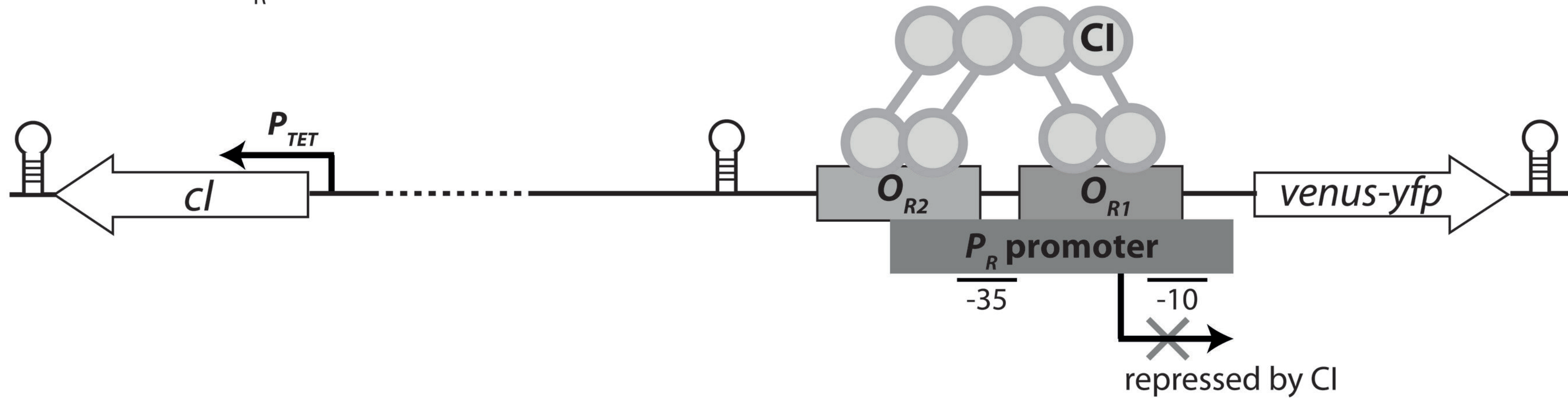
767 **Figure 6 – Source Data 1. Fluorescence measurements of single and double mutants, and**  
768 **the calculated values for epistasis for the validation mutant library.** Multiplicative epistasis,  
769 both in the absence and in the presence of the repressor CI, for each double mutant from  
770 the 30-mutant validation library, is provided along with the standard deviation for the  
771 measurement, the t-test value (5 degrees of freedom), and the FDR-corrected P value.  
772 Double mutants that do not exhibit a significant epistatic interaction are marked in green.  
773 Wildtype normalized fluorescence measurement of each single and double mutant, from  
774 which the epistasis values were calculated, is also provided for both environments.



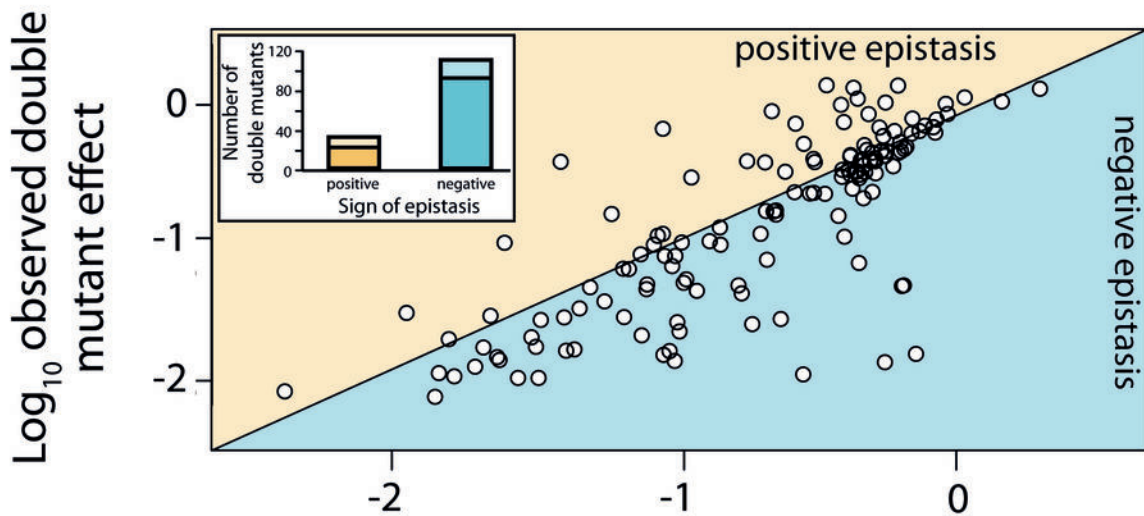
**a)** Experimental  $P_R$  system in the absence of CI



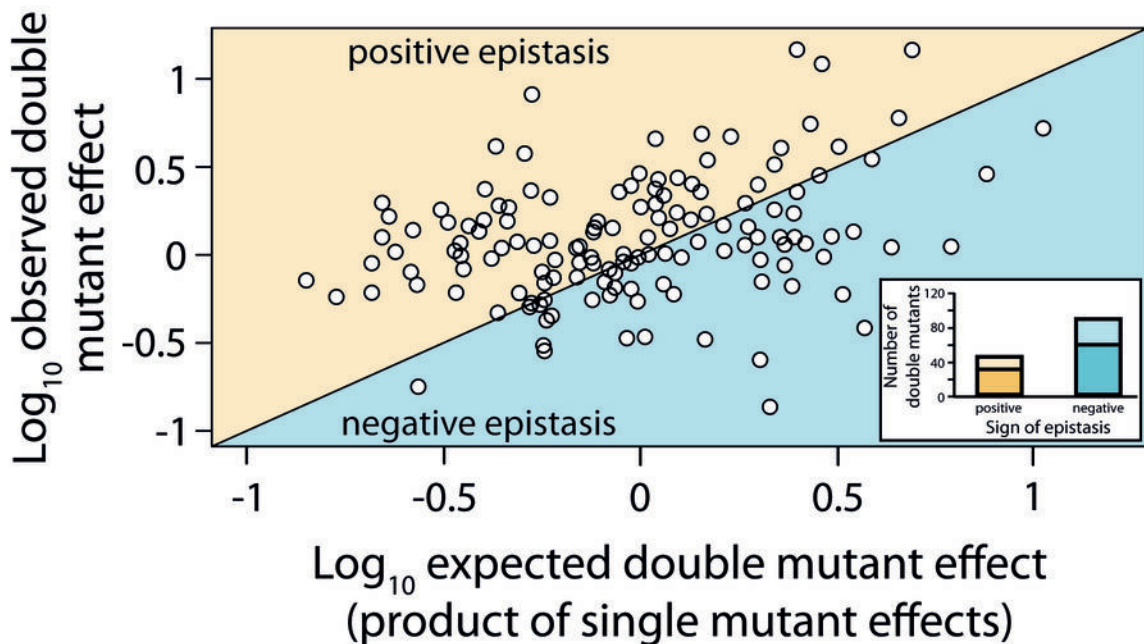
**b)** Experimental  $P_R$  system in the presence of CI



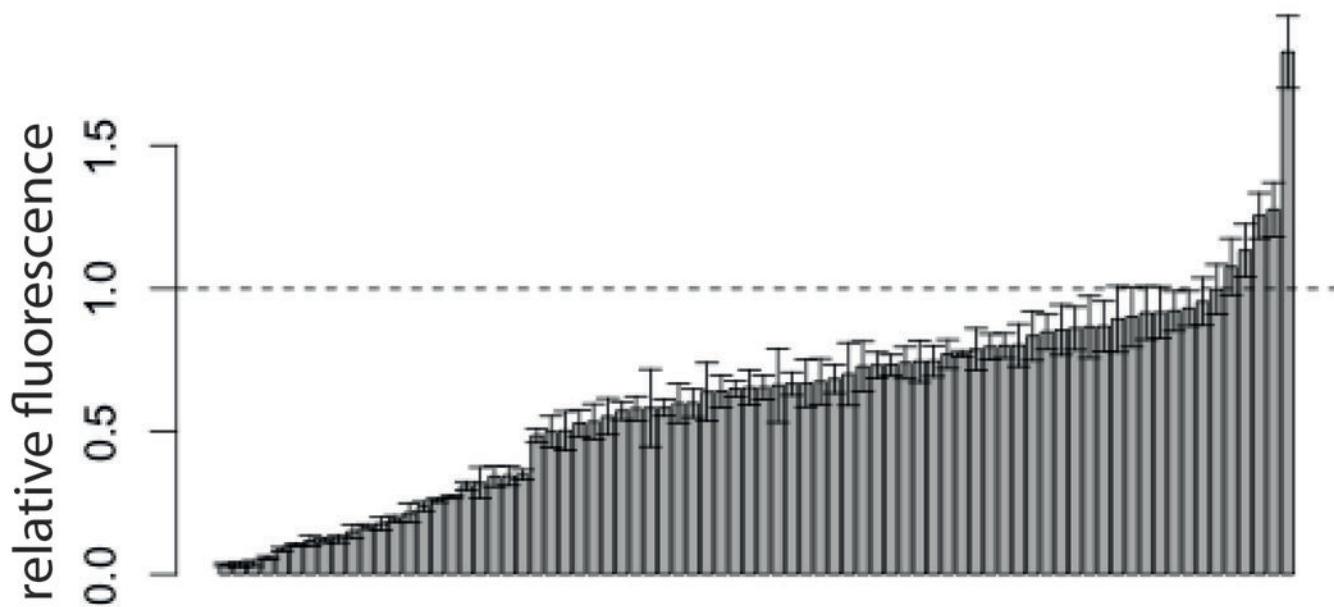
## a) Epistasis in the absence of CI



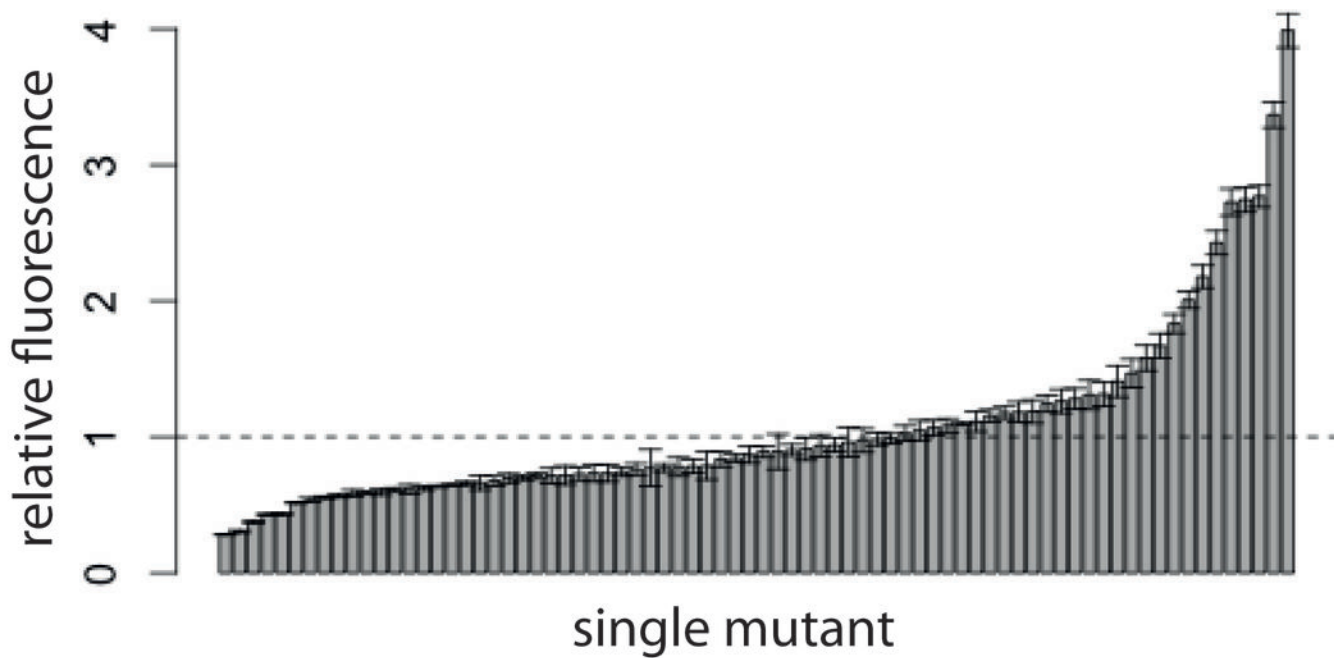
## b) Epistasis in the presence of CI



a) relative fluorescence in the absence of CI

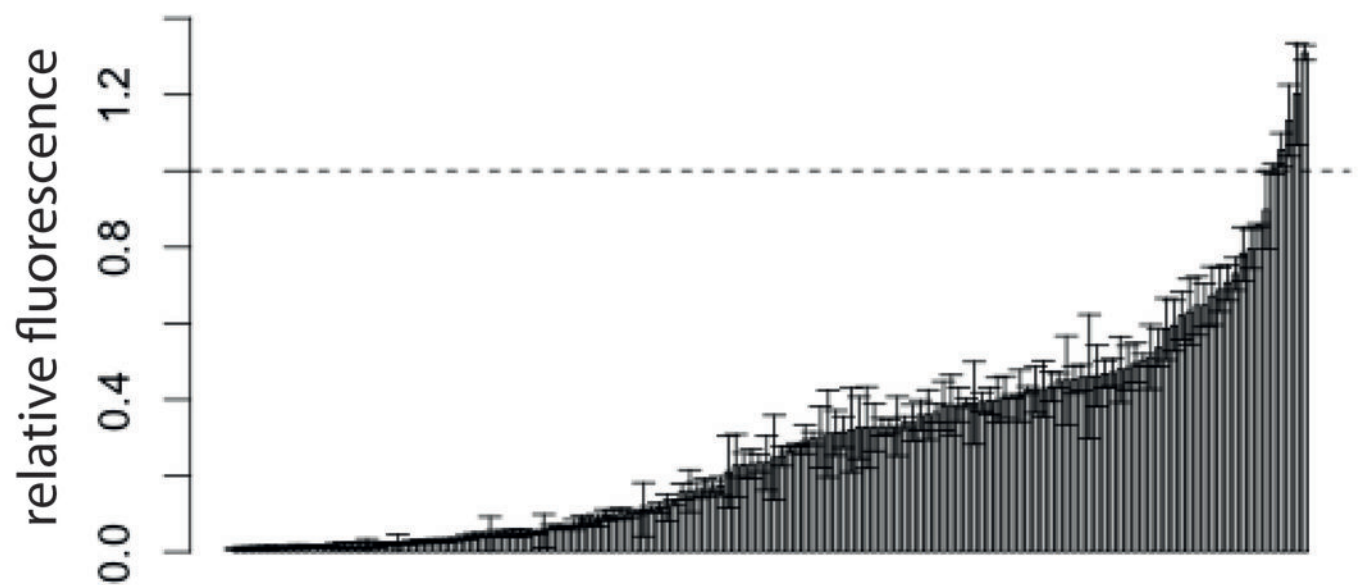


b) relative fluorescence in the presence of CI

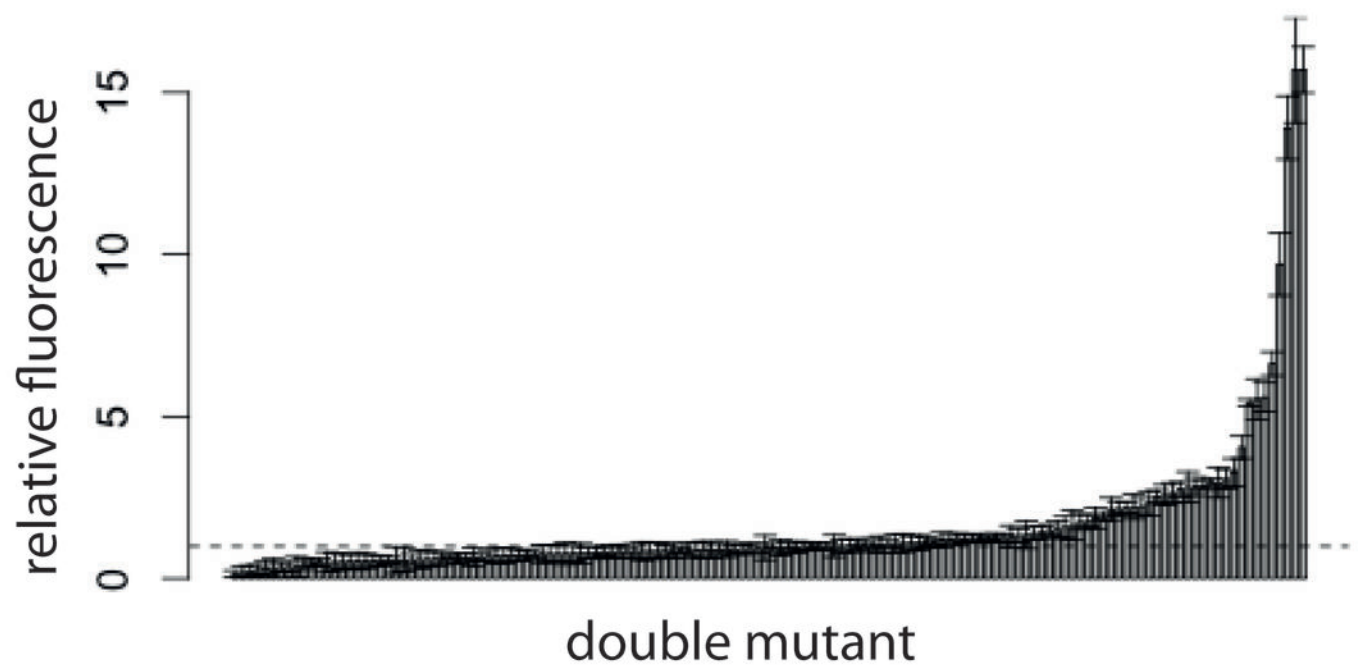




a) relative fluorescence in the absence of CI

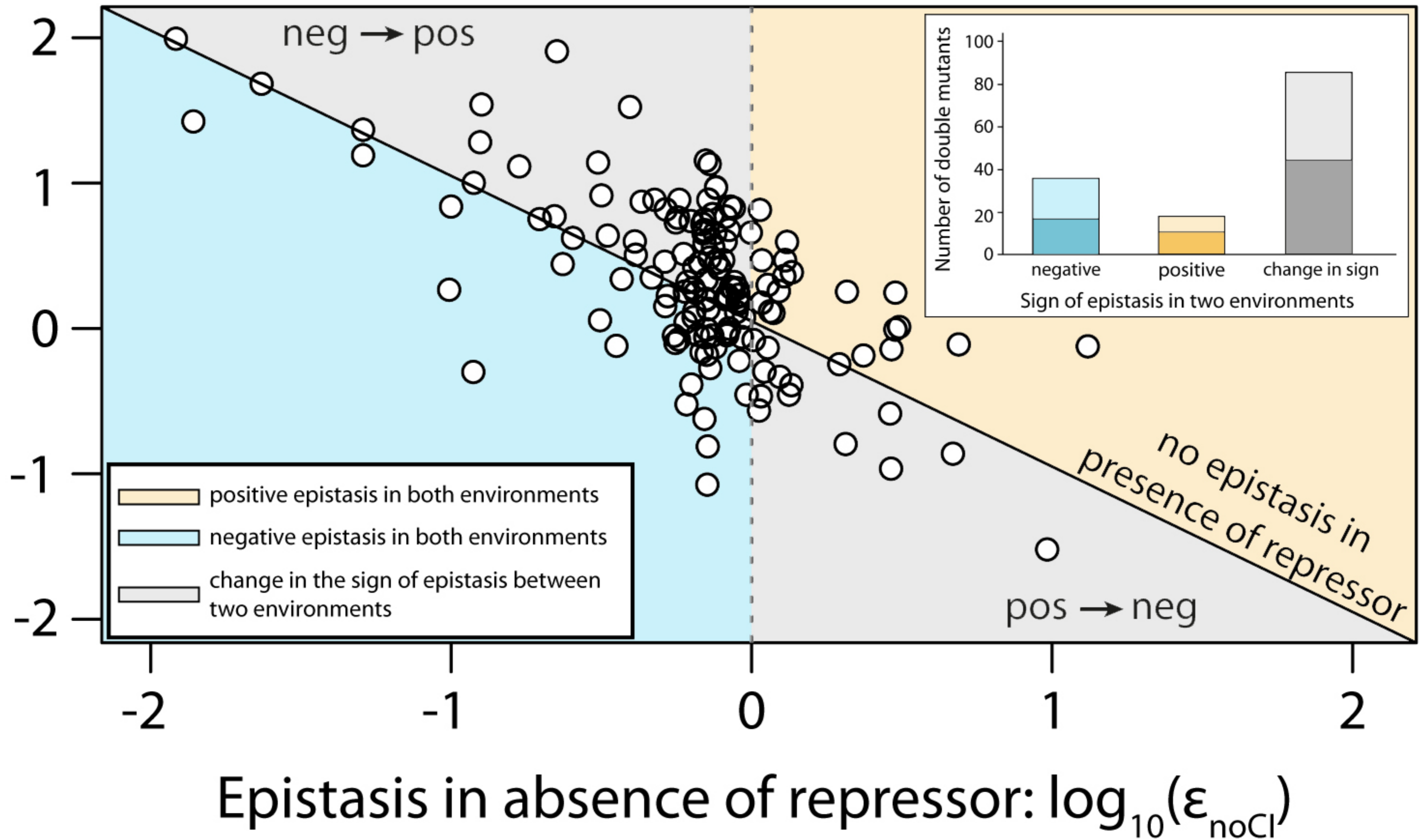


b) relative fluorescence in the presence of CI



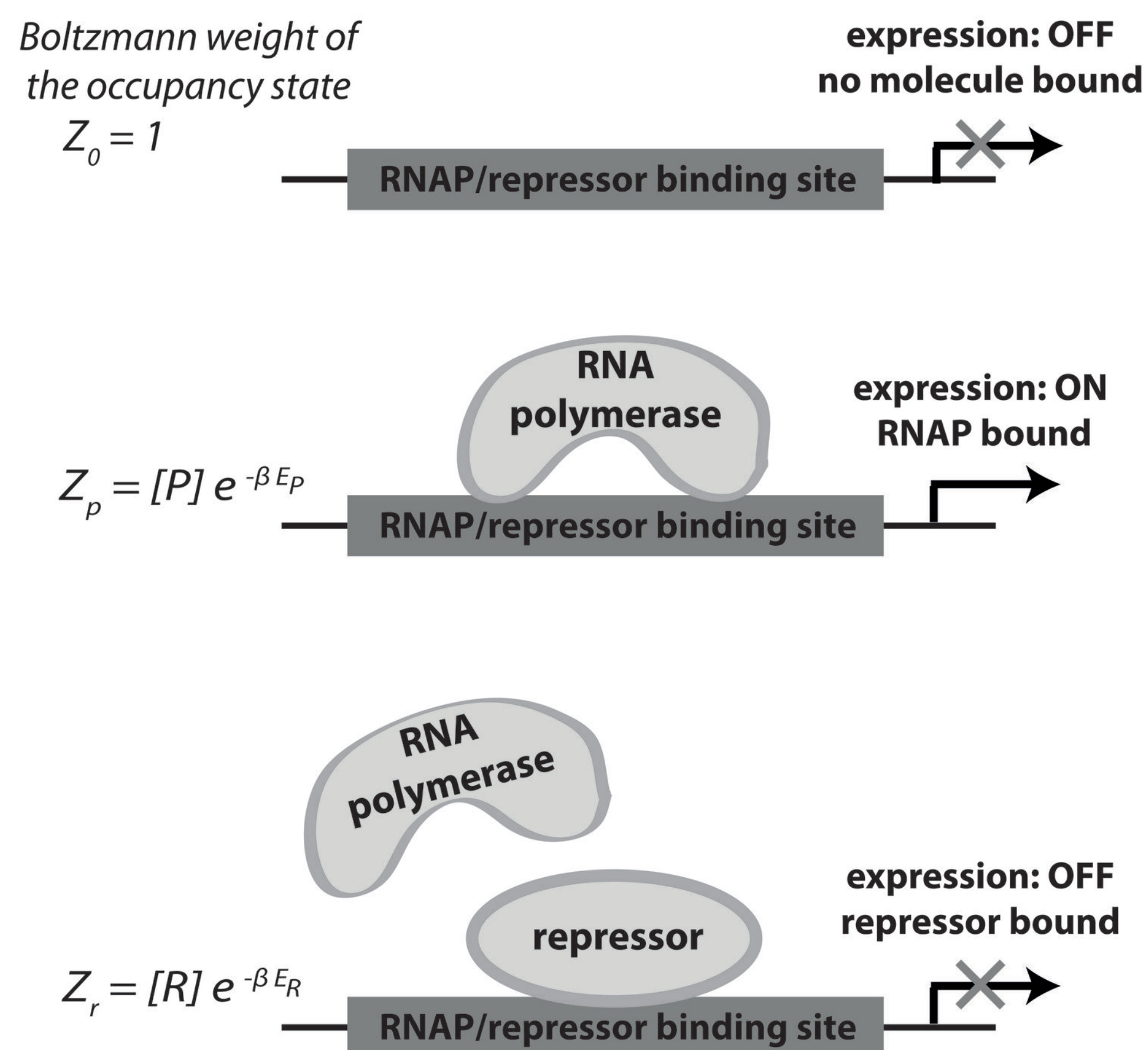
# Difference in epistasis:

$$\log_{10}(\varepsilon_{Cl}) - \log_{10}(\varepsilon_{noCl})$$

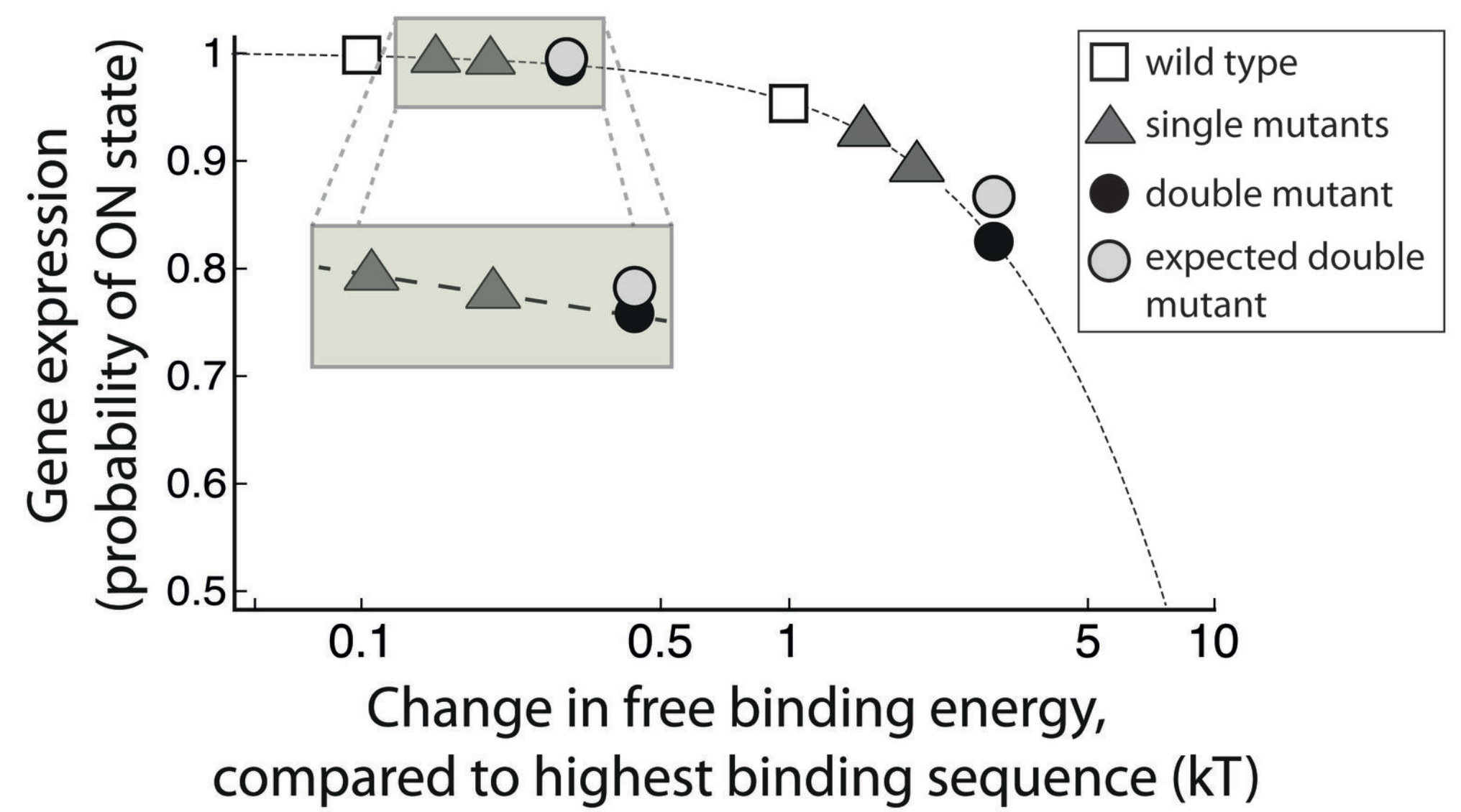




**a) Possible occupancy states in the thermodynamic model of gene regulation by binding-site competition**



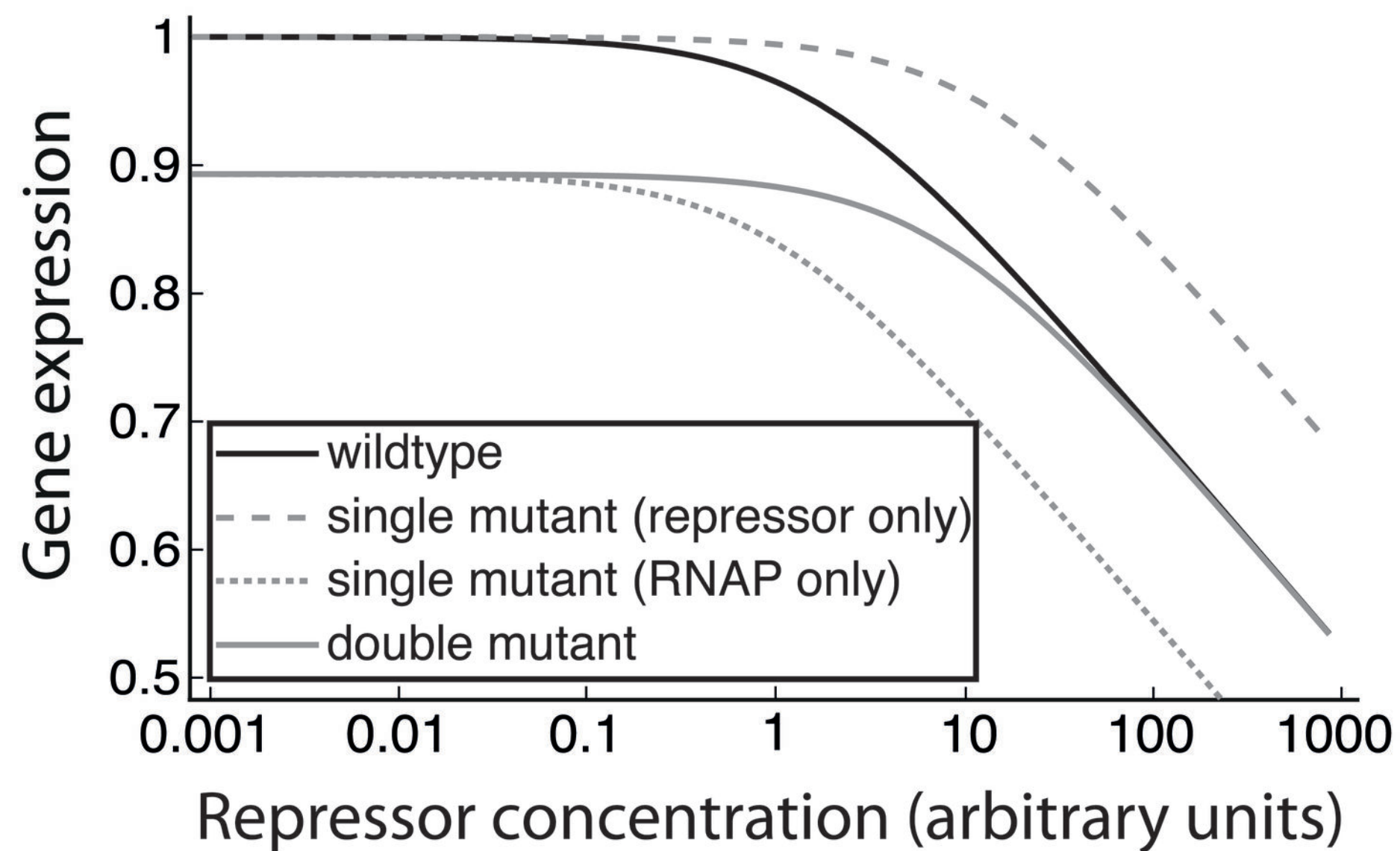
**b) Predictions of epistasis from the thermodynamic model**



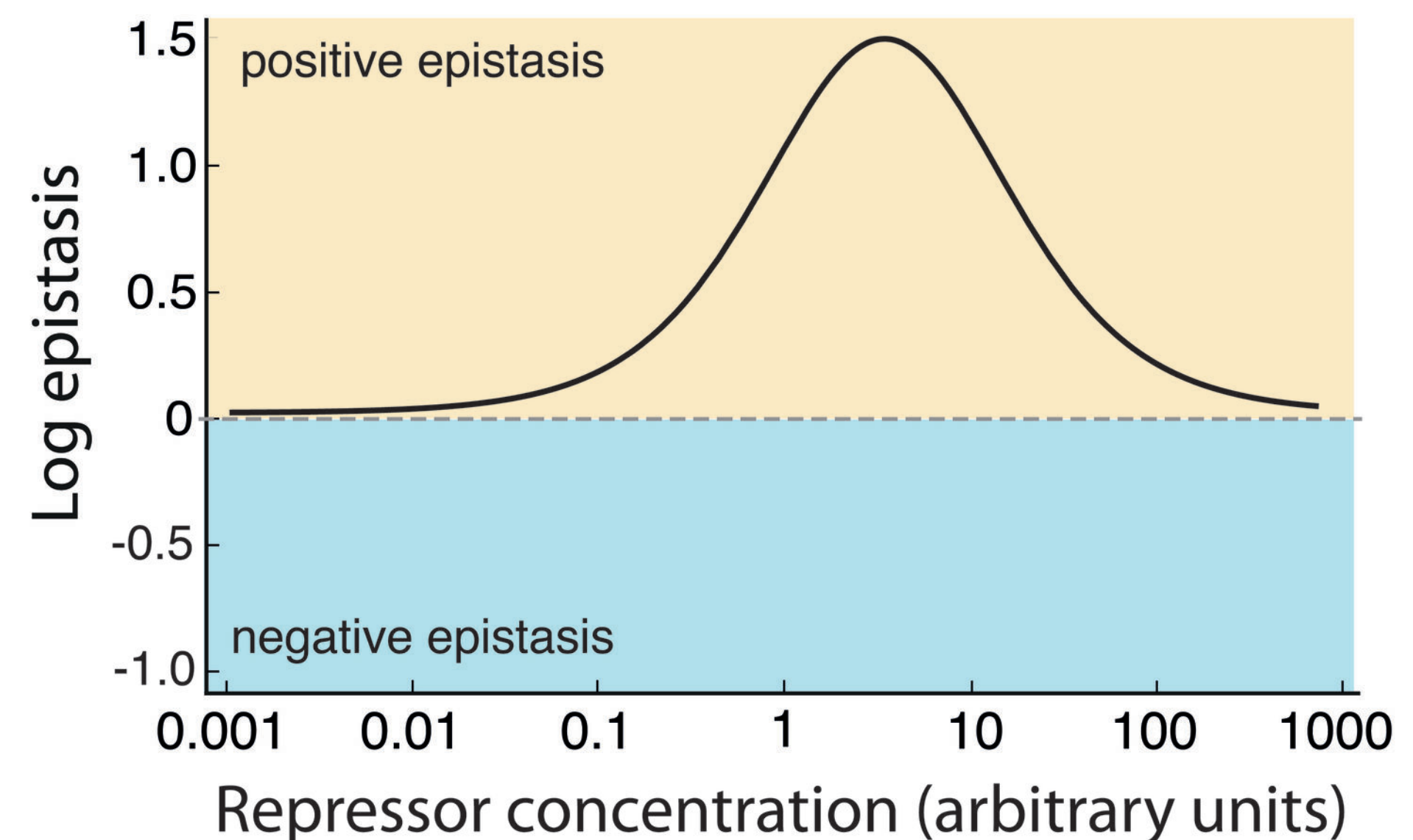
**c) Thermodynamic model predicts that sign of epistasis depends on sign of individual mutation effects**

		$p_1$	
		-	+
$p_2$	-	always negative	always positive
	+	always positive	always negative

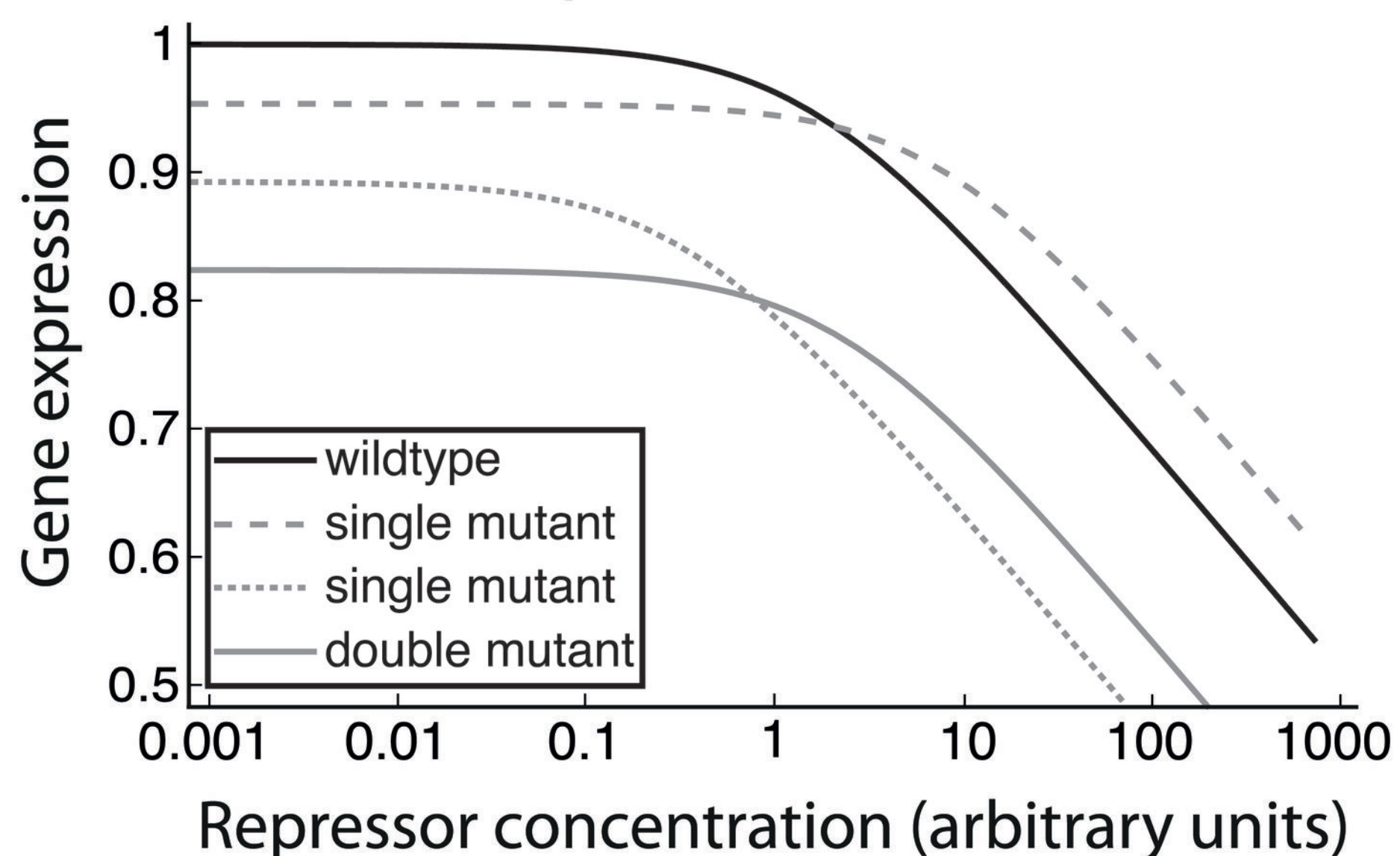
**d) Expression when single mutants affect only RNAP or repressor**



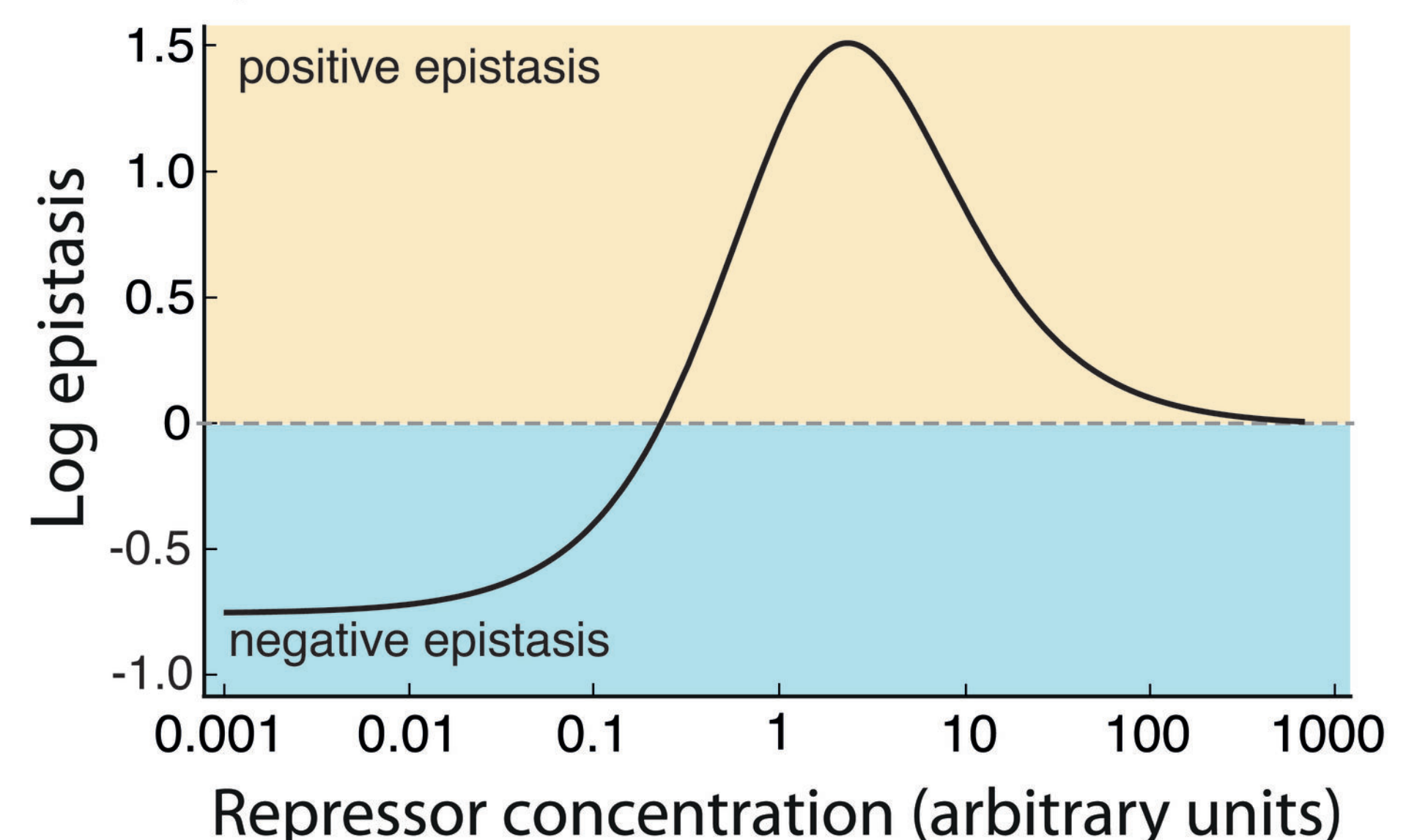
**e) Epistasis when single mutants affect only RNAP or repressor**



**f) Expression when single mutants affect both RNAP and repressor**



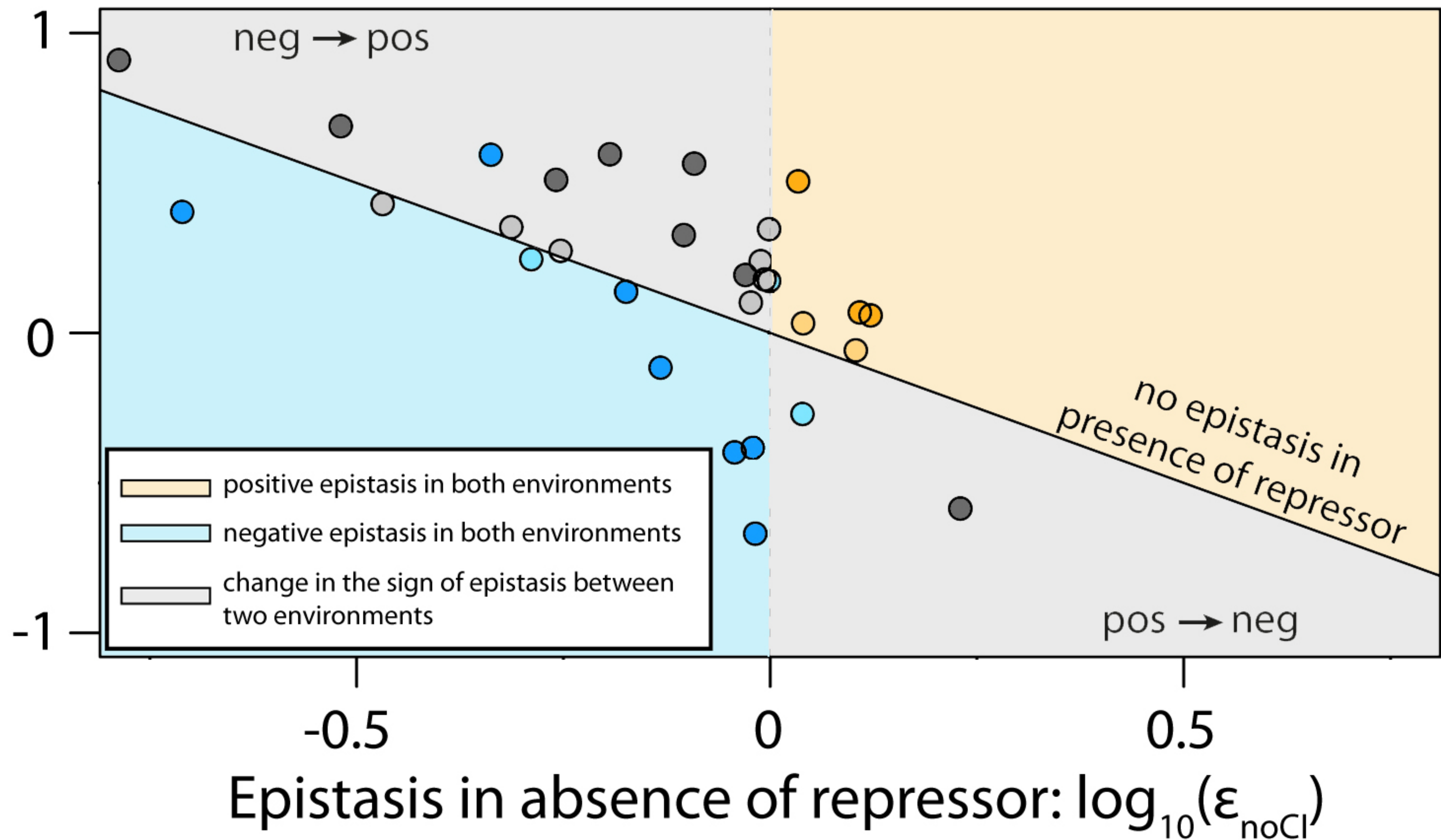
**g) Epistasis when single mutants affect both RNAP and repressor**



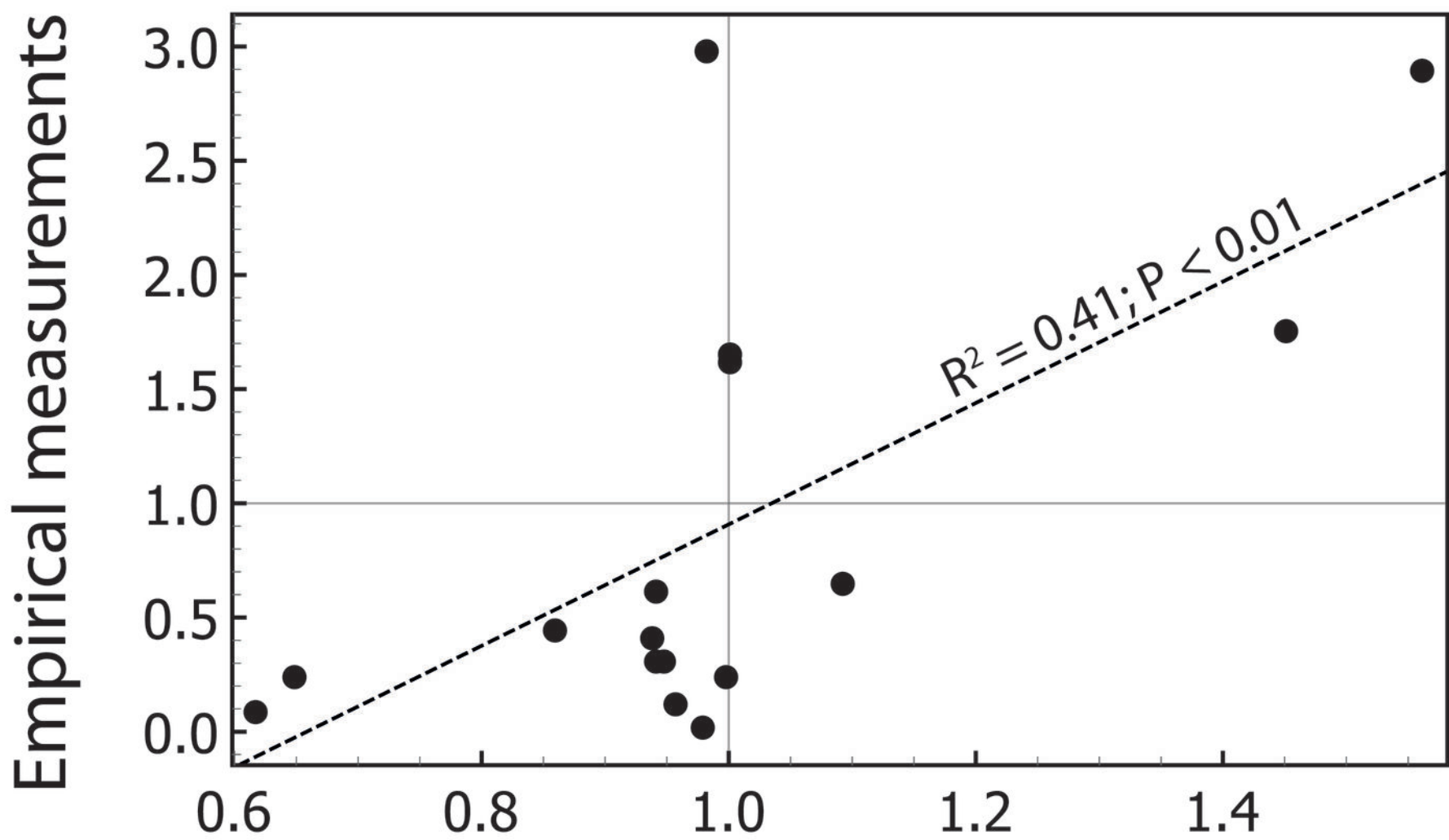


Difference in epistasis:

$$\log_{10}(\varepsilon_{Cl}) - \log_{10}(\varepsilon_{noCl})$$



## a) Absence of CI



## b) Presence of CI

